

Article

The Parotoid Gland Secretion from Peruvian Toad *Rhinella horribilis* (Wiegmann, 1833): Chemical Composition and Effect on the Proliferation and Migration of Lung Cancer Cells

Guillermo Schmeda-Hirschmann ^{1,*}, Jean Paulo de Andrade ^{1,2}, Marilú Roxana Soto-Vasquez ³, Paul Alan Arkin Alvarado-García ⁴, Charlotte Palominos ^{5,6}, Sebastián Fuentes-Retamal ^{5,6}, Mathias Mellado ^{5,6}, Pablo Correa ^{5,6} and Félix A. Urrea ^{5,6,*}

¹ Laboratorio de Química de Productos Naturales, Instituto de Química de Recursos Naturales, Universidad de Talca, Campus Lircay, Talca 3460000, Chile; jean.deandrade@utalca.cl

² Núcleo Científico Multidisciplinario, Dirección de Investigación, Universidad de Talca, Campus Lircay, Talca 3460000, Chile

³ Laboratorio de Farmacognosia, Facultad de Farmacia y Bioquímica, Universidad Nacional de Trujillo, Trujillo 13011, Peru; msoto@unitru.edu.pe

⁴ Facultad de Medicina, Universidad Privada Antenor Orrego, Trujillo 13001, Peru; palvaradog1@upao.edu.pe

⁵ Laboratorio de Plasticidad Metabólica y Bioenergética, Programa de Farmacología Clínica y Molecular, Instituto de Ciencias Biomédicas, Facultad de Medicina, Universidad de Chile, Santiago 8380453, Chile; palominos.ch@gmail.com (C.P.); sebastianfuentesr@gmail.com (S.F.-R.); mathignacionmellado@gmail.com (M.M.); pablo.correa.r@gmail.com (P.C.)

⁶ Network for Snake Venom Research and Drug Discovery, Santiago 7800003, Chile

* Correspondence: schmeda@utalca.cl (G.S.-H.); felixurraf@u.uchile.cl (F.A.U.); Tel.: +56-712-200-288 (G.S.-H.); +56-22-978-6066 (F.A.U.)

Received: 17 August 2020; Accepted: 9 September 2020; Published: 22 September 2020



Abstract: Since *Rhinella* sp. toads produce bioactive substances, some species have been used in traditional medicine and magical practices by ancient cultures in Peru. During several decades, the *Rhinella horribilis* toad was confused with the invasive toad *Rhinella marina*, a species documented with extensive toxicological studies. In contrast, the chemical composition and biological effects of the parotoid gland secretions (PGS) remain still unknown for *R. horribilis*. In this work, we determine for the first time 55 compounds from the PGS of *R. horribilis*, which were identified using HPLC-MS/MS. The crude extract inhibited the proliferation of A549 cancer cells with IC₅₀ values of 0.031 ± 0.007 and 0.015 ± 0.001 µg/mL at 24 and 48 h of exposure, respectively. Moreover, it inhibited the clonogenic capacity, increased ROS levels, and prevented the etoposide-induced apoptosis, suggesting that the effect of *R. horribilis* poison secretion was by cell cycle blocking before of G2/M-phase checkpoint. Fraction B was the most active and strongly inhibited cancer cell migration. Our results indicate that the PGS of *R. horribilis* are composed of alkaloids, bufadienolides, and argininy diacids derivatives, inhibiting the proliferation and migration of A549 cells.

Keywords: *Rhinella horribilis*; toad toxins; Peru; cell migration; proliferation; etoposide; bufadienolides

Key Contribution: This is the first comprehensive analysis of the chemical composition of parotoid gland secretions of *Rhinella horribilis*, a species previously confused with *R. marina*.

1. Introduction

Toads are widely distributed in the different biotas of Peru with a higher number of species in the Amazonian and eastern Andes [1,2] and are less frequent in the dry coastal ecosystems. Toads were known by the Native Americans both for their role in controlling insects as well as by their toxic defense substances. These toad toxins are secreted from parotoid glands that in contact with oral mucosa or eyes can produce intoxication or death [3–5]. Ceramic representations of *Rhinella* toad species by Peruvian pre-Inca Chavin and Moche cultures [6,7] and current local magic traditions in northern Peru that involved these toads (Figure 1A,B) suggest the presence of bioactive compounds. Currently, no studies are reporting the chemical composition and biological effects of the parotid glands secretions (PGS) of *Rhinella* sp. toads of the northern coast of Peru. The PGS of South American toads include alkaloids, argininy diacids, bufadienolides, and argininy diacid derivatives from bufadienolides. The biological effects from these secretions include cardiotoxic, cytotoxic, and antiproliferative activities, sometimes with a remarkable and selective effect on several cancer cell lines [8–10].

Non-small cell lung cancer (NSCLC) is the leading cause of cancer-related deaths globally [11]. The NSCLC tumors have high molecular heterogeneity, exhibiting gene mutations in B-Raf proto-oncogene, serine/threonine kinase (*BRAF*), *KRAS* proto-oncogene, and activating mutations of epidermal growth factor receptor (EGFR) [12]. Although recent advances in the development of new therapeutic strategies are focused on the reduction of proliferation and tumor growth [13,14]; reduced efforts have been put into identifying anti-invasive and anti-migratory drugs [15]. Promising uses of microtubule-targeting agents (MTA) have been proposed for NSCLC treatment in advanced stages [13]. Beyond the known effects of MTA on cell cycle progression, the blocking the microtubules stabilization by these anti-cancer drugs produces disruption of cell protrusions and cytoskeleton, triggering inhibition of tumor-induced angiogenesis and cancer cell migration/invasion [16].

Previously, we and others have described that the PGS of *Rhinella* species produces inhibition of proliferation by cell cycle arrest and induction of apoptosis [9,17,18], being the bufadienolides a promising source of anti-cancer chemical scaffolds [19]. The South American toad defense secretions consist of a complex mixture of argininy diacids, bufadienolides argininy diacids, bufadienolides, indolealkylamines, and peptides. The components less investigated so far are the peptides. Bioactive peptides also are considered a potential class of anticancer natural products, which inhibit cancer proliferation [20,21], angiogenesis [22], and induce selective apoptosis [23].

Little is known on the PGS composition and bioactivity of toad defensive compounds for the western South American Andes. No information is available on the secretion constituents of the recently known species of the northern Peru *Rhinella horribilis* (Figure 1C), which was extensively confused with *Rhinella marina* [24], a highly invasive species with well-known toxicological effects and bioactivities [8,18,25,26].

In this work, we report for the first time the chemical composition of the PGS from the Peruvian toad *R. horribilis* and describe the effect of the whole secretion and their main fractions on human lung cancer cells.



Figure 1. Representations of *Rhinella* species in traditional medicine and magical practices in Peru: (A) frogs and lizards on sale at the “Mercado de Brujos” (Witch’s market), Chichlayo, Peru; (B) Moche ceramic representing a frog; (C) adult specimen of *Rhinella horribilis* (Wiegmann, 1833), Peru; (D) thin layer chromatographic analysis (TLC) of the Sephadex LH-20 permeation showing the fraction pools A (FA; 27–30), B (FB; 31–38), and C (FC; 39–57) of PGS from *R. horribilis*. Adsorbent: silica gel; solvent system: EtOAc:isopropanol: NH_4OH (9:7:4). The plate was sprayed with a freshly prepared *p*-anisaldehyde solution reagent followed by heating up to 105 °C for maximum visualization of spots.

2. Results and Discussion

2.1. Fractionation of Parotoid Gland Secretions of *R. horribilis*

The crude secretions were fractionated into a group of constituents according to molecular size by permeation on Sephadex LH-20. The sample (660 mg) was loaded into a Sephadex LH-20 column (column length: 28.5 cm; internal diameter: 3.5 cm; filled with Sephadex® LH-20, Merck KGaA, Darmstadt, Germany). The eluent was methanol:chloroform (1:1). The void volume was 300 mL and 95 fractions of 3 mL each were collected. After TLC analysis (solvent system: ethanol:isopropanol:ammonium hydroxide 9:7:4 *v/v/v*), fractions with similar patterns were pooled as follows: fraction 11–26 (182.6 mg), fraction 27–30 (96.6 mg), fraction 31–38 (116.8 mg), fraction 39–57 (77.3 mg), fraction 58–69 (12 mg), and fraction 70–95 (12 mg) (Figure 1D). The pooled fractions

containing most of the constituents were further analyzed by ^1H NMR to obtain structural information on the group of compounds and for further examination by HPLC-MS/MS.

2.2. ^1H NMR Analysis

The ^1H NMR spectrum of the fractions 27–30 (Pool A) showed the characteristic signals for the H-21, H-22, and H-23 protons of the bufadienolide α -pyrone ring at δ 7.37–7.48, 7.86–8.00, and 6.25–6.32 ppm, respectively. Minor compounds of the pool presented a singlet at δ 9.67, 9.58, and 9.48 ppm, corresponding to an aldehyde function. The less abundant bufadienolides in the complex mixture displayed a singlet or broad singlet at δ 10.10, 10.08, 10.07, and 10.03 ppm, compatible with a second group of oxidized derivatives with an aldehyde group. According to Kamano et al. [27], the aldehyde signal resonates at δ 10.06 ppm for hellebrigenin and δ 9.49 ppm for resibufagin. The ^1H NMR spectrum of our sample supports the presence of a mixture of compounds belonging mainly to the bufalin and marinobufagin series, with the aldehydes and further oxidized bufadienolides as minor constituents. The main bufadienolides in the fraction are marinobufagin and bufalin argininy diacids. The HPLC-MS/MS analysis (Section 2.3) confirmed the occurrence of several hellebrigenin and resibufagin argininy diacids, supporting the NMR assignments. The Pool B, including fractions 31–38, shows a mixture of argininy diacids, free bufadienolides, and minor amounts of bufadienolides argininy diacids. The main groups of the components were resibufagin, telocinobufagin, marinobufagin, bufalin, and resibufogenin derivatives. The identity was established by HPLC-MS/MS analysis (see Section 2.3). The ^1H NMR analysis of the fraction 39–57 (Pool C) showed a main compound with H signals at δ 7.32 d (8.4) (1H), 7.12 s (1H), 6.86 d (8.4) (1H), 4.02 br t (5.6) (2H), 3.71 s (6H) and 3.31 ppm (br t, 5.6), in agreement with dehydrobufotenine (DHB) (compound A2). Additional signals support the presence of a mixture of argininy diacids and minor amounts of bufadienolides. HPLC-MS/MS analysis of the fraction confirmed the occurrence of DHB as the main constituent and the presence of adipyl-, pimeloyl- and suberoylarginine. The ^1H NMR analysis of the pool of fractions 58–69 and 70–95 showed the characteristic signals for a mixture of argininy diacids and was not further investigated.

2.3. HPLC-DAD-Q-TOF-MS/MS Analysis

The crude PGS and the main fraction pools A, B, and C were analyzed by high performance liquid chromatography (HPLC) coupled to a diode-array detector (DAD) and to a quadrupole time-of-flight mass spectrometry/mass spectrometry detector (Q-TOF-MS/MS) to identify the constituents of the complex mixtures (Table 1). Detected and calculated $[\text{M}+\text{H}]^+$ ions were compared and the error was calculated for the tentative identification of the different compounds. Data analyses followed previous work on toad poison secretions [9,10,18,28–31].

2.3.1. Compounds Identified: Argininy Diacids

In the HPLC-MS/MS analysis (Table 1 and Figure 2), six compounds eluting in the first third of the chromatographic run showed the loss of a diacid from the positively charged ion and arginine at m/z 175 as the common amino acid in the structural series. The difference in the compounds 1–6 (Figure 3) was the number of CH_2 units in the diacid moiety. The compounds were identified as adipoyl-, pimeloyl-, suberoyl-, azeloyl-, sebacyl- and undecadienoyl arginine, respectively. Argininy diacids were described in the poison secretions of other South American *Rhinella* species, including *R. marina* [18], *R. schneideri* [9,10], *R. ornata* and *R. scitula* [9]. For all argininy diacids and *N*-diacid argininy bufadienolides, extracted ion chromatograms at m/z 303, 317, 331, 345, 359 and 373 allowed to confirm the occurrence of adipyl-, pimeloyl-, suberoyl-, azeloyl-, sebacyl- and undecadienoyl arginine esters, respectively.

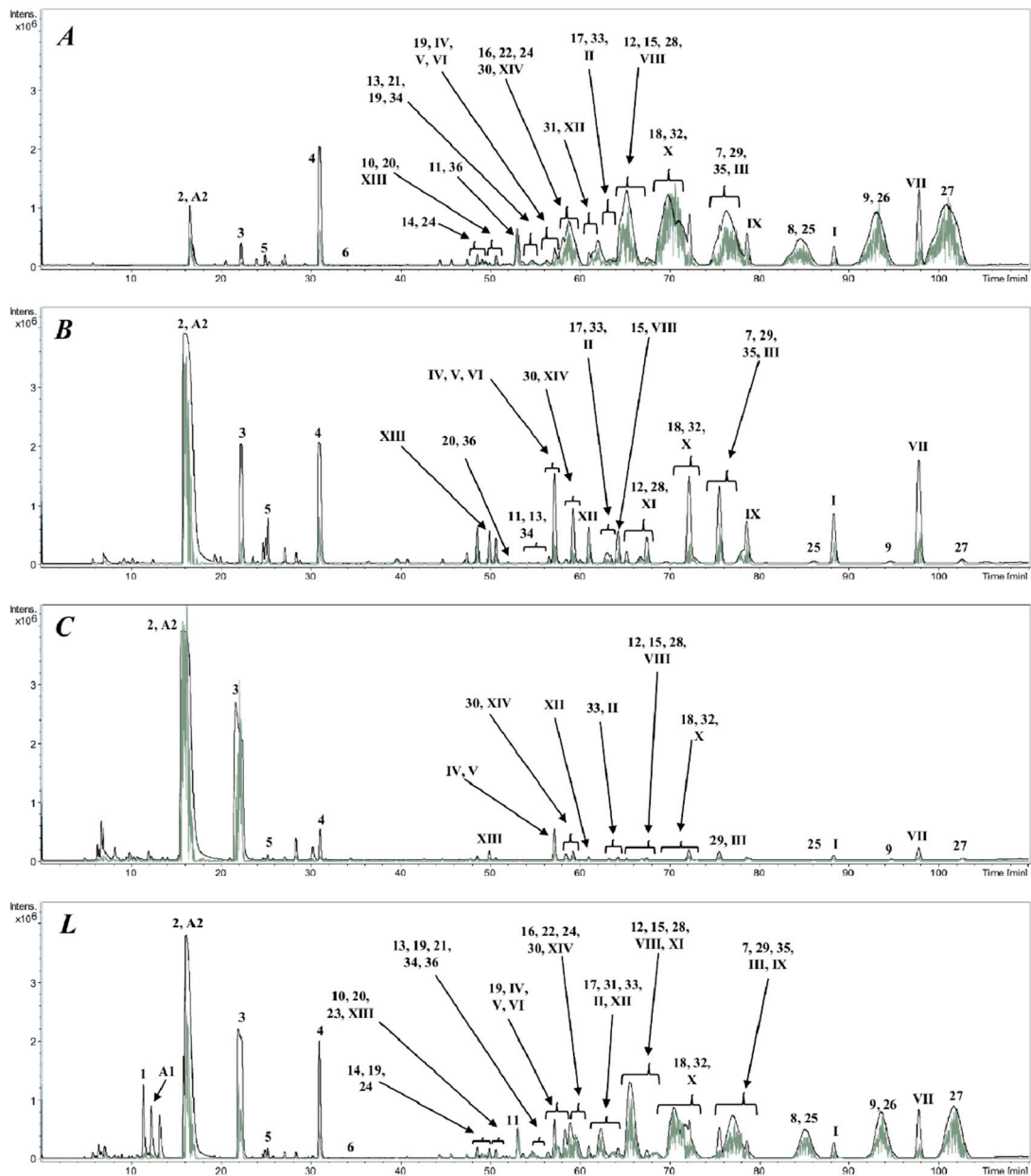


Figure 2. HPLC-MS/MS chromatogram of the fractions 27–30 (A), 31–38 (B), 39–57 (C), and the lyophilized crude extract (L) of the parotoid gland secretions from Peruvian *Rhinella horribilis*. Total ion current (TIC) (black line) and MS² (gray line). Detection in the positive ion mode.

Table 1. HPLC-MS/MS data (positive ion mode) of the defense compounds of the lyophilized crude extract of parotoid gland secretion (L) from the Peruvian *Rhinella horribilis* and the fractions 27–30 (A), 31–38 (B), and 39–57 (C). Abbreviations: N° = compound number, for the structures see Figures 3–5; Rt = Retention time; Sample: fractions 27–30 (A), 31–38 (B), 39–57 (C), lyophilized crude extract (L).

N°	Rt (min)	Sample	[M+H] ⁺ Detected	[M+H] ⁺ Expected	Error (ppm)	MS/MS Fragmentation	Tentative Identification
1	11.4–11.9	L	303.1624	303.1663	12.8	303.1624 (<1), 244.1169 (32), 222.1210 (14), 175.1184 (27), 158.0852 (22), 130.1935 (14), 128.0688 (26), 116.0685 (100), 95.0600 (39).	Adipoyl arginine C ₁₂ H ₂₃ N ₄ O ₅ ⁺ [28]
A1	12.8	L	176.0685	176.0666	10.8	176.0688 (<1), 159.0660 (17), 143.0720 (9), 133.0536 (16), 117.0560 (52), 115.0533 (100), 115.0533 (100), 105.0673 (31), 89.0368 (17)	Guanidinosuccinic acid C ₅ H ₁₀ N ₃ O ₄ ⁺ [28]
2	15.6–17.0	A, B, C, L	317.1804	317.1819	4.7	317.1804 (<1), 273.4732 (40), 194.1169 (52), 158.0895 (65), 125.0623 (87), 112.0849 (100)	Pimeloyl arginine C ₁₃ H ₂₅ N ₄ O ₅ ⁺ [28]
A2	15.7–17.2	A, B, C, L	203.1178	203.1179	0.5	203.1178 (<1), 188.0932 (50), 173.0708 (100), 145.0764 (9), 118.0667 (10), 89.0364 (16)	Dehydrobufotenine C ₁₂ H ₁₅ N ₂ O ⁺ [28]
3	21.8–22.7	A, B, C, L	331.1962	331.1976	4.2	331.1980 (20), 272.1486 (100), 172.1057 (86), 125.0603 (48), 112.0879 (46)	Suberoyl arginine C ₁₄ H ₂₇ N ₄ O ₅ ⁺ [28]
5	25.2–25.5	A, B, C, L	359.2260	359.2289	8.0	359.2366 (21), 272.1458 (100), 246.4343 (17), 226.1422 (20), 203.1506 (33), 116.0996 (35)	Sebacyl arginine isomer C ₁₆ H ₃₁ N ₄ O ₅ ⁺ [28]
4	30.9–31.5	A, B, C, L	345.2123	345.2132	2.6	345.2100 (19), 286.1628 (27), 250.1529 (85), 175.1197 (58), 158.0932 (44), 139.0761 (42), 116.0709 (100)	Azelayl arginine C ₁₅ H ₂₉ N ₄ O ₅ ⁺ [28]
6	34.0–34.1	A, L	373.2417	373.2445	8.3	373.2341 (34), 286.1592 (100), 254.1458 (30), 203.1485 (40), 172.1096 (40), 116.0702 (75)	Undecadienoyl arginine C ₁₇ H ₃₃ N ₄ O ₅ ⁺ [28]
24	48.8–49.3	A, L	745.4000	745.4018	2.4	745.3983 (78), 727.3875 (13), 434.7749 (6), 331.1942 (100), 313.1949 (11), 278.1473 (33), 250.1558 (25), 195.1161 (17), 158.0890 (17), 117.0713 (31), 112.0840 (58), 91.0538 (27)	3-(N-suberoyl argininy)l Hydroxyhellebrigenin isomer 1 C ₃₈ H ₅₇ N ₄ O ₁₁ ⁺ [28,29]
19	49.1–49.2	L	731.4225	731.4226	0.1	331.1932 (100), 314.1670 (18), 278.1441 (25), 175.1128 (10)	3-(N-suberoyl argininy)l Hellebrigenol isomer 1 C ₃₈ H ₅₉ N ₄ O ₁₀ ⁺ [28]
14	49.3–49.7	A, L	715.3888	715.3913	3.5	715.3906 (40), 697.3787 (5), 363.1930 (5), 345.1796 (2), 317.1788 (100), 264.1340 (7), 175.1181 (4), 112.0878 (11)	3-(N-pimeloyl argininy)l Desacetylcinobufotalin C ₃₇ H ₅₅ N ₄ O ₁₀ ⁺ [32]
10	49.8–50.1	A, L	687.3952	687.3964	1.7	687.3984 (46), 669.3618 (4), 385.2361 (5), 303.1627 (100), 268.1292 (11), 250.1171 (13), 105.0685 (12)	3-(N-adipoyl argininy)l Gamabufotalin C ₃₆ H ₅₅ N ₄ O ₉ ⁺ [28,32]
XIII	50.6–50.9	A, B, C, L	417.2262	417.2272	2.4	417.2286 (100), 399.2198 (18), 381.2053 (50), 363.1946 (34), 345.1840 (33), 209.0929 (62), 165.0687 (62), 103.0526 (89), 91.0544 (94)	Arenobufagin C ₂₄ H ₃₃ O ₆ ⁺ [31].
23	50.8–50.9	L	731.3845	731.3862	2.3	731.3845 (35), 439.2103 (11), 317.1809 (100), 300.1562 (16), 264.1334 (20), 178.0778 (9), 155.0880 (13)	3-(N-pimeloyl argininy)l Hydroxyhellebrigenin C ₃₇ H ₅₅ N ₄ O ₁₁ ⁺ [28]
20	51.5–51.7	A, B, L	701.3741	701.3756	2.1	701.3747 (96), 683.3639 (11), 665.3641 (2), 381.2004 (3), 364.1916 (5), 363.1984 (4), 335.1984 (18), 317.1910 (3), 303.1640 (100), 268.1239 (14), 250.1194 (17), 175.1192 (3), 129.0689 (16), 91.0528 (31)	3-(N-adipoyl argininy)l Hellebrigenin C ₃₆ H ₅₃ N ₄ O ₁₀ ⁺ [32]
36	52.1–52.4	A, B, L	743.3854	743.3862	2.3	743.3860 (100), 725.3687 (7), 377.1703 (9), 331.1968 (99), 278.1481 (26), 250.1546 (23), 175.1230 (7), 165.0706 (14), 128.0629 (22), 112.0881 (24), 910533 (25)	3-(N-suberoyl argininy)l Hydroxybufotalinin isomer 1 C ₃₈ H ₅₅ N ₄ O ₁₁ ⁺ [28]

Table 1. Cont.

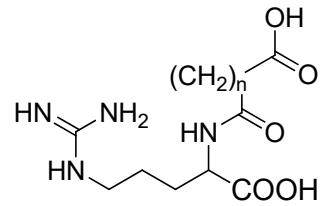
N°	Rt (min)	Sample	[M+H] ⁺ Detected	[M+H] ⁺ Expected	Error (ppm)	MS/MS Fragmentation	Tentative Identification
11	53.3–54.1	A, B, L	701.4062	701.4120	8.2	701.4080 (95), 683.3979 (2), 385.2287 (4), 317.1767 (100), 264.1285 (33), 236.1363 (8), 105.0669 (20)	3-(N-pimeloyl argininy) Gamabufotalin C ₃₇ H ₅₇ N ₄ O ₉ ⁺ [28]
21	54.1–55.0	A, L	715.3879	715.3913	4.8	715.3864 (100), 697.3839 (7), 669.3725 (3), 381.2027 (5), 364.1992 (1), 363.1928 (5), 651.3676 (6), 353.2058 (2), 345.1816 (3), 335.2013 (8), 317.1787 (71), 282.1417 (8), 264.1309 (14), 236.1364 (9), 175.1165 (8), 112.0861 (23), 105.0702 (17), 91.0535 (27)	3-(N-pimeloyl argininy) Hellebrigenin C ₃₇ H ₅₅ N ₄ O ₁₀ ⁺ [32]
19	54.2–54.6	A, L	731.4171	731.4226	7.5	731.4143 (72), 363.1946 (12), 331.1891 (100), 278.1446 (35), 250.1450 (15), 175.1177 (17), 112.0873 (23)	3-(N-suberoyl argininy) Hellebrigenol isomer 2 C ₃₈ H ₅₉ N ₄ O ₁₀ ⁺
13	54.3–54.8	A, B, L	701.3728	701.3756	4.0	701.3721 (100), 684.3766 (1), 610.9012 (1), 399.2135 (6), 381.2023 (2), 353.2069 (2), 335.1959 (1), 303.1635 (89), 286.1387 (9), 268.1256 (15), 250.1156 (17), 175.1180 (11), 116.0692 (16), 112.0878 (15), 105.0691 (13), 91.0537 (10)	3-(N-adipoyl argininy) Arenobufagin C ₃₆ H ₅₃ N ₄ O ₁₀ ⁺ [32]
36	54.7–54.9	A, L	743.3825	743.3862	4.9	743.3829 (65), 349.1888 (8), 331.1935 (100), 296.1560 (9), 278.1480 (25), 250.1528 (55), 233.0955 (4), 179.0855 (11), 112.0869 (34), 91.0555 (22)	3-(N-suberoyl argininy) Hydroxybufotalin isomer 2 C ₃₈ H ₅₅ N ₄ O ₁₁ ⁺ [28]
34	55.1–55.4	A, B, L	713.3706	713.3756	7.0	713.3715 (100), 695.3598 (3), 667.3739 (4), 317.1781 (88), 300.1509(22), 282.1434(12), 264.1334 (12), 236.1370 (16), 209.0860 (5), 179.0818 (10), 175.1225 (7), 112.0855 (35), 91.0524 (43)	3-(N-pimeloyl argininy) Bufotalin C ₃₇ H ₅₃ N ₄ O ₁₀ ⁺ [28]
VI	56.5–56.7	A, B, L	419.2400	419.2428	6.6	419.2400 (5), 401.2318 (30), 365.2088 (63), 347.2036 (36), 319.1615 (33), 213.1616 (27), 91.0531 (51)	Hellebrigenol C ₂₄ H ₃₅ O ₆ ⁺ [32]
IV or V	57.0–57.6	A, B, C, L	417.2244	417.2272	6.7	417.2226 (100), 399.2122 (35), 371.2176 (4), 353.2056 (3), 335.1972 (5), 255.0976 (2), 175.0722 (4)	Bufarenogin or ψ-Bufarenogin C ₂₄ H ₃₃ O ₆ ⁺ [32]
19	57.0–57.8	A, L	731.4184	731.4226	5.7	731.4189 (55), 713.4048 (5), 683.3909 (10), 665.3843 (4), 331.1919 (100), 278.1468 (10), 250.1475 (9), 175.1179 (4), 112.0854 (20)	3-(N-suberoyl argininy) Hellebrigenol isomer 3 C ₃₈ H ₅₉ N ₄ O ₁₀ ⁺ [28]
16	57.9–58.2	A, L	687.3947	687.3964	2.4	687.3960 (27), 669.3813 (7), 303.1641 (100), 250.1177 (13), 175.1446 (8), 145.0968 (14), 91.0533 (17)	3-(N-adipoyl argininy) Telocinobufagin C ₃₆ H ₅₅ N ₄ O ₉ ⁺ [28]
24	58.1–58.4	A, L	745.4001	745.4018	2.3	745.4017 (11), 683.4230 (11), 345.2155 (10), 331.1923 (100), 303.1952 (8), 278.1492 (10), 175.1148 (15), 112.0836 (35)	3-(N-suberoyl argininy) Hydroxyhellebrigenin isomer 2 C ₃₈ H ₅₇ N ₄ O ₁₁ ⁺ [28]
30	58.3–59.0	A, B, C, L	685.3780	685.3807	3.9	685.3757 (28), 669.3790 (5), 667.3653 (3), 365.2086 (3), 349.2058 (4), 303.1615 (100), 268.1240 (12), 250.1140 (12), 175.1140 (6), 105.0678 (13)	3-(N-adipoyl argininy) Marinobufagin C ₃₆ H ₅₃ N ₄ O ₉ ⁺ [28]
22	58.4–60.0	A, L	729.4021	729.4069	6.5	729.4010 (100), 711.3899 (8), 693.3760 (2), 683.3970 (2), 363.1912 (4), 331.1926 (68), 278.1459 (16), 250.1516 (16), 175.1188 (8), 112.0861 (27), 91.0534 (27)	3-(N-suberoyl argininy) Hellebrigenin C ₃₈ H ₅₇ N ₄ O ₁₀ ⁺ [28,29]
XIV	59.0–59.6	A, B, C, L	417.2242	417.2272	7.2	417.2244 (62), 399.2122 (26), 363.1903 (30), 353.2077 (26), 335.1959 (73), 317.1874 (10), 275.1754 (16), 211.1433 (33), 128.0608 (71), 91.0527 (100)	Hellebrigenin C ₂₄ H ₃₃ O ₆ ⁺ [28]
31	60.5–64.3	A, L	699.3980	699.3964	2.3	699.3971 (38), 681.3823 (7), 365.2102 (4), 347.2001 (4), 317.1806 (100), 264.1314 (11), 236.1361 (6), 175.1198 (5), 112.0883 (10), 91.0523 (10)	3-(N-pimeloyl argininy) Marinobufagin C ₃₇ H ₅₅ N ₄ O ₉ ⁺ [28]

Table 1. Cont.

N°	Rt (min)	Sample	[M+H] ⁺ Detected	[M+H] ⁺ Expected	Error (ppm)	MS/MS Fragmentation	Tentative Identification
XII	60.8–61.4	A, B, C, L	415.2092	415.2115	5.5	415.2085 (22), 379.1865 (8), 361.1792 (12), 351.1927 (30), 333.1820 (26), 237.1619 (28), 165.0669 (30), 128.0609 (64), 115.0530 (79), 91.0534 (100)	Bufotalinin C ₂₄ H ₃₁ O ₆ ⁺ [32]
17	62.4–64.7	A, B, L	701.4097	701.4120	3.3	701.4087 (24), 683.3955 (5), 349.2203 (3), 317.1786 (100), 264.1308 (5), 236.1406 (3), 175.1172 (3), 105.0711 (8)	3-(N-pimeloyl argininyl) Telocinobufagin C ₃₇ H ₅₇ N ₄ O ₉ ⁺ [28]
33	62.7–63.7	A, B, C, L	683.3682	683.3651	3.6	683.3613 (100), 665.3521 (2), 335.1963 (4), 303.1635 (40), 286.1371 (9), 268.1273 (8), 250.1161 (17), 226.1057 (3), 175.1187 (5), 112.0873 (13)	3-(N-adipoyl argininyl) Marinobufagin-9,11-ene C ₃₆ H ₅₁ N ₄ O ₉ ⁺
II	62.9–63.4	A, B, C, L	403.2453	403.2479	6.4	403.2445 (30), 385.2335 (58), 349.2120 (44), 337.2111 (41), 275.1742 (25), 253.1888 (39), 241.1922 (49), 161.0968 (29), 105.0785 (46), 91.0546 (100)	Gamabufotalin C ₂₄ H ₃₅ O ₅ ⁺ [28,32]
VIII	64.0–64.7	A, B, C, L	401.2312	401.2323	2.7	401.2295 (34), 383.2866 (3), 365.2081 (15), 347.1970 (20), 337.2165 (14), 319.2024 (10), 257.1163 (21), 239.1059 (32), 211.1096 (27), 183.1154 (24), 128.0626 (86), 105.0700 (85), 91.0547 (100)	Resibufaginol C ₂₄ H ₃₃ O ₅ ⁺ [31]
15	64.4–66.5	A, B, C, L	729.4052	729.4069	2.3	729.4077 (100), 399.2156 (5), 381.2065 (2), 363.1959 (2), 353.2100 (1), 345.1862 (1), 335.1983 (2), 331.1959 (83), 278.1487 (25), 250.1541 (18), 175.1200 (11), 112.0875 (27)	3-(N-suberoyl argininyl) Desacetylcinobufotalin C ₃₈ H ₅₇ N ₄ O ₁₀ ⁺ [29]
12	66.4–67.2	A, B, C, L	715.4254	715.4277	3.2	715.4250 (80), 697.4150 (12), 349.2108 (4), 331.1936 (100), 314.1679 (12), 278.1462 (32), 250.1514 (24), 175.1165 (9), 116.0691 (22), 91.0531 (16)	3-(N-suberoyl argininyl) Gamabufotalin C ₃₈ H ₅₉ N ₄ O ₉ ⁺ [28]
XI	66.5–66.7	B, L	415.2090	415.2115	6.0	415.2054 (100), 397.1832 (3), 333.1887 (3), 283.1621 (5), 253.0760 (5), 175.0999 (6)	19-Oxo-desacetylcinobufagin C ₂₄ H ₃₁ O ₆ ⁺ [28]
28	66.5–69.5	A, B, C, L	697.3766	697.3807	5.9	697.3745 (100), 679.3595 (2), 363.1933 (3), 335.1966 (4), 317.1759 (61), 264.1290 (33), 236.1349 (11), 175.1154 (4)	3-(N-pimeloyl argininyl) Resibufagin C ₃₇ H ₅₃ N ₄ O ₉ ⁺ [28]
18	68.6–72.0	A, B, C, L	715.4265	715.4277	1.7	715.4266 (44), 697.4156 (7), 349.2136 (4), 331.1944 (100), 314.1708 (3), 278.1484 (8), 250.1538 (5), 175.1193 (4), 105.0695 (11), 91.0540 (11)	3-(N-suberoyl argininyl) Telocinobufagin C ₃₈ H ₅₉ N ₄ O ₉ ⁺ [28]
32	70.0–72.6	A, B, C, L	713.4101	713.4120	2.6	713.4100 (48), 695.3992 (5), 365.2075 (3), 331.1941 (100), 314.1681 (5), 296.1581 (3), 278.1473 (12), 250.1533 (8), 175.1198 (8), 112.0873 (16), 91.0536 (15)	3-(N-suberoyl argininyl) Marinobufagin C ₃₈ H ₅₇ N ₄ O ₉ ⁺ [28]
X	71.8–72.6	A, B, C, L	399.2150	399.2166	4.0	399.2150 (<1), 381.2104 (24), 363.2394 (14), 331.1949 (35), 275.1786 (19), 239.1741 (52), 213.1297 (33), 128.0661 (46), 115.0554 (42), 105.0684 (67), 91.0533 (100)	Resibufagin C ₂₄ H ₃₁ O ₅ ⁺ [32]
29	74.6–78.9	A, B, C, L	711.3941	711.3964	1.1	711.3956 (100), 363.1933 (3), 331.1937 (40), 278.1463 (24), 250.1522 (18), 175.1179 (14)	3-(N-suberoyl argininyl) Resibufagin C ₃₈ H ₅₅ N ₄ O ₉ ⁺ [28]
7	74.6–75.8	A, B, L	671.4014	671.4014	0.0	671.4048 (64), 653.3916 (8), 351.2269 (5), 303.1638 (100), 286.1403 (6), 250.1151 (18), 175.1213 (3), 158.0926 (4), 105.0691 (13), 91.0525 (14)	3-(N-adipoyl argininyl) bufalin C ₃₆ H ₅₅ N ₄ O ₈ ⁺ [28]
III	75.1–76.0	A, B, C, L	403.2464	403.2479	3.7	403.2456 (57), 385.2353 (37), 367.2252 (44), 349.2135 (79), 253.1929 (31), 215.1780 (30), 105.0700 (79), 91.0537 (100)	Telocinobufagin C ₂₄ H ₃₅ O ₅ ⁺ [29,31]
35	76.4–77.5	A, B, L	727.3922	727.3913	4.0	727.3917 (100), 711.3898 (6), 397.1995 (9), 331.1962 (100), 278.1494 (35), 250.1532 (29), 175.1180 (21), 112.0885 (34), 91.0540 (23)	3-(N-suberoyl argininyl) Bufotalinin C ₃₈ H ₅₅ N ₄ O ₁₀ ⁺ [28]
IX	78.3–79.2	A, B, L	401.2323	401.2323	0.0	401.2335 (23), 383.2235 (10), 365.2105 (51), 347.2012 (32), 337.2162 (17), 319.2068 (19), 269.1890 (20), 253.1938 (44), 251.1797 (31), 239.1061 (22), 183.1157 (25), 128.0639 (74), 105.0710 (81), 91.0543 (100)	Marinobufagin C ₂₄ H ₃₃ O ₅ ⁺ [32]

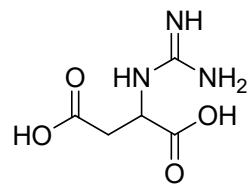
Table 1. Cont.

N°	Rt (min)	Sample	[M+H] ⁺ Detected	[M+H] ⁺ Expected	Error (ppm)	MS/MS Fragmentation	Tentative Identification
25	82.6–86.3	A, B, C, L	669.3840	669.3858	2.7	669.3835 (100), 349.2124 (2), 303.1628 (79), 286.1395 (5), 268.1264 (14), 250.1156 (24), 175.1188 (8), 116.0695 (11), 91.0531 (6)	3-(N-adipoyl argininy) Resibufogenin C ₃₆ H ₅₃ N ₄ O ₈ ⁺ [28]
8	83.0–86.2	A, L	685.4142	685.4171	4.2	685.4113 (94), 667.4030 (11), 351.2260 (7), 317.1779 (100), 300.1539 (10), 264.1298 (24), 175.1181 (9), 112.0860 (22), 91.0520 (20)	3-(N-pimeloyl argininy) bufalin C ₃₇ H ₅₇ N ₄ O ₈ ⁺ [28]
I	87.8–88.7	A, B, C, L	387.2512	387.2530	4.6	387.2482 (60), 369.2396 (72), 351.2291 (52), 333.2204 (10), 255.2101 (57), 187.1454 (14), 173.1330 (16), 128.0637 (36), 105.0698 (88), 91.0541 (100)	Bufalin C ₂₄ H ₃₅ O ₄ ⁺ [31]
26	91.4–94.6	A, L	683.4000	683.4014	2.0	683.4015 (100), 665.3974 (2), 349.2114 (5), 317.1791 (83), 300.1531 (11), 282.1435 (11), 264.1338 (25), 236.1358 (13), 175.1163 (10), 143.0834 (6), 112.0868 (16), 91.0546 (12)	3-(N-pimeloyl argininy) Resibufogenin C ₃₇ H ₅₅ N ₄ O ₈ ⁺ [28]
9	91.4–95.1	A, B, C, L	699.4313	699.4327	2.0	699.4311 (100), 681.4213 (14), 351.2279 (6), 331.1942 (78), 314.16814 (9), 296.1568 (6), 278.1477 (21), 250.1522 (14), 175.1169 (9), 112.0863 (21), 91.0541 (15)	3-(N-suberoyl argininy) bufalin C ₃₈ H ₅₉ N ₄ O ₈ ⁺ [28]
VII	97.3–98.3	A, B, C, L	385.2328	385.2373	7.7	385.2318 (8), 367.2221 (15), 349.2133 (12), 321.2151 (6), 253.1923 (19), 241.1195 (14), 205.0860 (16), 185.0928 (4), 115.0544 (49), 105.0689 (69), 91.0531 (100)	Resibufogenin C ₂₄ H ₃₃ O ₄ ⁺ [29,32]
27	98.7–103.1	A, B, C, L	697.4117	697.4171	7.7	697.4110 (100), 679.4003 (2), 349.2108 (3), 331.1917 (85), 314.1667 (7), 278.1455 (26), 250.1503 (19), 175.1157 (9), 112.0854 (19), 910525 (11)	3-(N-suberoyl argininy) Resibufogenin C ₃₈ H ₅₇ N ₄ O ₈ ⁺ [28]

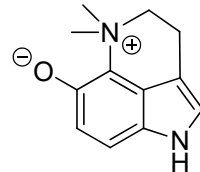


Arginyl diacid derivatives

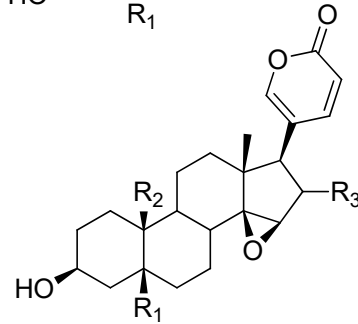
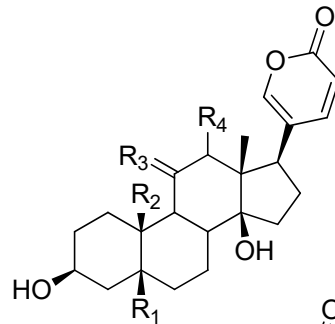
Compd	n	Diacid
1	4	Adipic acid
2	5	Pimelic acid
3	6	Suberic acid
4	7	Azelaic acid
5	8	Sebacic acid
6	9	Undecadienoic acid



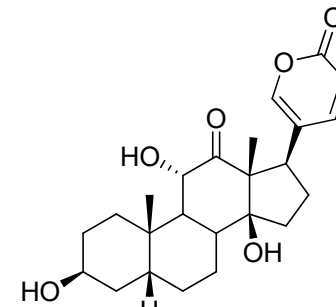
A1 Guanidosuccinic acid



A2 Dehydrobufotenine



I	$R_1=H, R_2=CH_3, R_3=H_2, R_4=H$	Bufalin
II	$R_1=H, R_2=CH_3, R_3=OH,H; R_4=H$	Gamabufotalin
III	$R_1=OH, R_2=CH_3, R_3=H_2, R_4=H$	Telocinobufagin
IV	$R_1=H, R_2=CH_3, R_3=H_2, R_4=\beta OH$	Bufarenogin
V	$R_1=H, R_2=CH_3, R_3=H_2, R_4=\alpha OH$	ψ -Bufarenogin
VI	$R_1=OH, R_2=CH_2OH, R_3=H_2, R_4=H$	Hellebrigenol
XIV	$R_1=OH, R_2=CHO, R_3=H_2, R_4=H$	Hellebrigenin
VII	$R_1=H, R_2=CH_3, R_3=H$	Resibufogenin
VIII	$R_1=H, R_2=CH_2OH, R_3=H$	Resibufaginol
IX	$R_1=OH, R_2=CH_3, R_3=H$	Marinobufagin
X	$R_1=H, R_2=CHO, R_3=H$	Resibufagin
XI	$R_1=H, R_2=CHO, R_3=OH$	19-Oxo-desacetylcinobufagin
XII	$R_1=OH, R_2=CHO, R_3=H$	Bufotalinin
XV	$R_1=OH, R_2=CH_3, R_3=OH$	Desacetylcinobufotalin



XIII Arenobufagin

Figure 3. Structure of the compounds A1, A2, genines (bufadienolides) I–XV, and arginyl diacids 1–6 tentatively identified in PGS of *R. horribilis*.

2.3.2. Alkaloids and Guanidine Derivatives

The alkaloid guanidinosuccinic acid (A1) and dehydrobufotenine (A2) were detected in the PGS (Figure 3). The fragmentation pattern and errors comparing the detected and expected mass fully support the identification. Dehydrobufotenin was reported in the PGS of *R. marina* and *R. schneideri* [9,18].

2.3.3. Bufadienolides

The bufadienolides bufalin (I), gamabufotalin (II), telocinobufagin (III), bufarenogin/ ψ -bufarenogin (IV, V), hellebrigenol (VI), resibufogenin (VII), resibufaginol (VIII), marinobufagin (IX), resibufagin (X), 19-oxo-desacetylcinobufagin (XI), bufotalinin (XII), arenobufagin (XIII), and hellebrigenin (XIV) were identified by comparing the molecular formula and fragmentation patterns with literature. According to Ye and Guo [29], resibufaginol (VIII) elutes before marinobufagin (IX) and, the elution sequence agrees with our assignment (Figure 3).

2.3.4. Argininyl Diacids of Bufadienolides

In the toad secretions, bufadienolides occur as free and as argininyl diacid derivatives. The identity of the bufadienolide moiety followed from the analysis of the neutral loss of water from the $[M+H]^+$ ion and subsequent fragmentation leading to the arginine ion at m/z 175. The neutral loss of 368 amu from the $[M+H]^+$ ion was used to identify the homologous series of bufalin derivatives. Compounds **7**, **8**, and **9** were identified as 3-(*N*-adipoylargininyl)-, 3-(*N*-pimeloylargininyl)- and 3-(*N*-suberoylargininyl) bufalin, respectively, in agreement with the literature [9]. The telocinobufagin derivatives, with an additional hydroxyl function at C-5, showed a constant neutral loss of 384 amu, as can be observed for the mass spectra of compounds **16–18**. While the identity of the argininyl diacid moiety can be unambiguously assigned, telocinobufagin and its isomer gamabufotalin, with a hydroxyl function at C-11 instead of C-5, show the same molecular formula and fragments. In the *R. horribilis* poison secretion, two compounds with the molecular formula $C_{36}H_{54}N_4O_9$ were detected at R_t 49.8–50.1 and 57.9–58.2 min; two products with the molecular formula $C_{37}H_{56}N_4O_9$ at R_t 53.3–54.1 and 62.4–64.7 min; and two compounds presenting the molecular formula $C_{38}H_{58}N_4O_9$ at R_t 66.4–67.2 and 68.6–72.0 min, and were assigned to the adipoyl- (compound **10** and **16**), pimeloyl- (**11** and **17**) and suberoyl- (compounds **12** and **18**) esters of gamabufotalin and telocinobufagin, respectively. According to Cao et al. [28] for argininyl diacids from gamabufotalin and telocinobufagin, the homologous series have higher R_t for the telocinobufagin than for the gamabufotalin argininyl diesters. Therefore, in the pairs with the same molecular formula and fragments, the compound with lower R_t was tentatively identified as the gamabufotalin argininyl ester. The same observation regarding R_t values is found for the genines by Ye and Guo [29] and Ren et al. [33]. Three compounds with molecular formula $C_{38}H_{58}N_4O_{10}$ eluted at R_t 49.1–49.2, 54.2–54.6 and 57.0–57.8 min and fragmented to the base peak at m/z 331, in agreement with 3-(*N*-suberoyl argininyl) hellebrigenol (compound **19**). The three compounds differ in the intensity of the ions after fragmentation and were assigned as suberoyl argininyl hellebrigenol isomers 1, 2, and 3, respectively (Figure 4).

Compounds **20–22** are isomers of the compounds **13–15**, differing in the placement of the hydroxy function (C-5 for **20–22**, C-11 for **13**, and C-5/C-16 for **14–15**). The compounds **14** and **15** present an epoxy function while there is a carbonyl ketone at C-12 in **13** and the aldehyde from hellebrigenin in compounds **20–22**. The compounds **20–22** were assigned as adipoyl-, pimeloyl- and suberoylargininyl hellebrigenin based on the neutral loss of 398 amu, leading to the peak of the argininyl diacids. 3-(*N*-suberoylargininyl) hellebrigenin (hellebritoxin) was reported from the PGS of *R. marina* from the Peruvian Amazon [18] and Paraguayan *Rhinella* species [9].

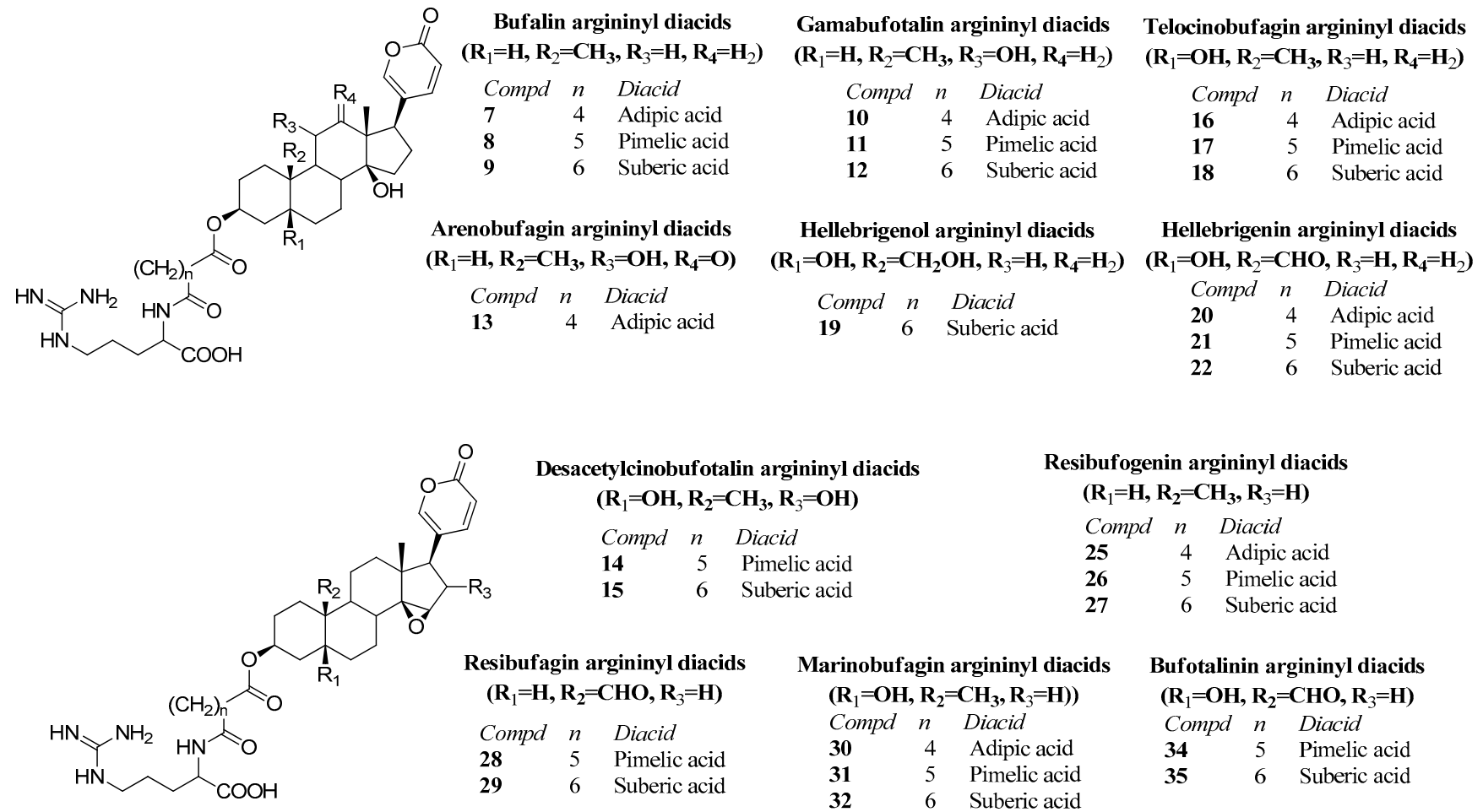


Figure 4. Structure of the compounds 7–22, 25–32, and 34–35 tentatively identified in the parotoid gland secretion of *R. horribilis*.

The occurrence of hellebrigenin and resibufagin argininyl diacids in our samples was suggested by the ^1H NMR analysis of the PGS and fractions. The isomer pairs with the molecular formula $\text{C}_{36}\text{H}_{52}\text{N}_4\text{O}_{10}$, $\text{C}_{37}\text{H}_{54}\text{N}_4\text{O}_{10}$, and $\text{C}_{38}\text{H}_{56}\text{N}_4\text{O}_{10}$, were assigned as 3-(*N*-adipoyl argininyl) arenobufagin **13** and 3-(*N*-adipoyl argininyl) hellebrigenin **20**; 3-(*N*-pimeloyl argininyl) desacetylcinobufotalin **14** and 3-(*N*-pimeloyl argininyl) hellebrigenin **21**; 3-(*N*-suberoyl argininyl) desacetylcinobufotalin **15** and 3-(*N*-suberoyl argininyl) hellebrigenin **22**, respectively. The assignment of the arenobufagin and hellebrigenin argininyl diacids in our samples of PGS follows the elution sequence previously reported for the genes and argininyl esters of both compounds, with hellebrigenin isomers eluting before the corresponding arenobufagin derivatives [33]. Ren et al. [33] reported that arenobufagin elutes before hellebrigenin in their PGS samples. Furthermore, the loss of 29 amu in the hellebrigenin derivatives was observed for compounds **20–22** in agreement with Ye and Guo [29] (Figure 4).

The compound **23** showed the neutral loss of 414 amu and a base peak in agreement with pimeloylarginine and was assigned as 3-(*N*-pimeloyl argininyl) hydroxyhellebrigenin. Two compounds with the same molecular formula $\text{C}_{38}\text{H}_{56}\text{N}_4\text{O}_{11}$ and R_t 48.8–49.3 and 58.1–58.4 min occur in the PGS. The mass spectrum of the compound, described here as compound **24**, showed the neutral loss of 414 amu, leading to the suberoylargininyl ion at m/z 331. The compound was assigned as 3-(*N*-suberoyl argininyl) hydroxyhellebrigenin. The placement of the additional hydroxyl function in compound **24** remains to be established, being C-12 or C-16 the most probable options. The isomers were tentatively identified as 3-(*N*-suberoyl argininyl) hydroxyhellebrigenin **24** isomer 1 and 2, respectively. The resibufogenin derivatives (compounds **25**, **26** and **27**) were assigned based on the loss of 366 amu from the $[\text{M}+\text{H}]^+$ ion, leading to the argininyl diacids and were identified as adipoyl-, pimeloyl- and suberoylresibufogenin, respectively. The compounds were previously reported from the Amazonian *R. marina* [18] and Paraguayan *Rhinella* species [9] (Figures 4 and 5).

The compounds **28**, **29**, **34**, and **35** were tentatively assigned by the neutral loss of the bufadienolide from the $[\text{M}+\text{H}]^+$ ions, leading to the argininyl esters. The compounds **28** and **29** with a neutral loss of 380 amu are compatible with the aldehyde derivatives of resibufogenin (resibufagin) and were assigned as pimeloylargininyl resibufagin **28** and suberoylargininyl resibufagin **29**, respectively. The compounds **34** and **35** showed the neutral loss of 396 amu in agreement with aldehyde derivatives of marinobufagin (bufotalin), being assigned as pimeloylargininyl bufotalin **34** and suberoylargininyl bufotalin **35**, respectively. The compounds **30**, **31**, and **32** showed the neutral loss of 382 amu, with base peak for adipoyl-, pimeloyl-, and suberoylarginine and were identified as marinobufagin argininyl diacids, in full agreement with spectrometric data reported for South American *Rhinella* species [10,18]. Marinobufagin is the 5-hydroxy derivative of resibufogenin. The compound **33**, with the molecular formula $\text{C}_{36}\text{H}_{50}\text{N}_4\text{O}_9$ shows one additional unsaturation than compound **30**, it presents the neutral loss of 380 amu and the base peak for adipoyl arginine. It was tentatively assigned as 3-(*N*-adipoyl argininyl) marinobufagin-9,11-ene **33**. Two compounds with the molecular formula $\text{C}_{38}\text{H}_{54}\text{N}_4\text{O}_{11}$ eluted at R_t 52.1–52.4 and 54.7–54.9 min, respectively, and showed the neutral loss of 412 amu, suggesting the occurrence of hydroxybufotalin derivatives differing in the placement of the hydroxyl group. For hydroxybufotalin, the most common hydroxylation places are either at C-11, C-12, or C-16. However, we are not able to fully assign the most probable isomers. The compound **36** was tentatively identified as 3-(*N*-suberoyl argininyl) hydroxybufotalin **36** isomers 1 and 2, respectively (Figures 4 and 5).

In this study, we identified a high number of constituents (55 compounds) from PGS of *R. horribilis* compared to the 29 compounds previously reported from three Peruvian Amazon populations of *R. marina* [18]. Although this difference might be explained by the different environments, access to food or the sensibility of the instrument used, we are not excluding the hypothesis of unique chemical composition patterns for both species. This is especially relevant if is considered that both *R. marina* and, previously confused *R. horribilis*, have geographical, genetic, and morphological differences [24,34]. The main compounds in the PGS are marinobufagin and bufalin derivatives, with aldehydes as minor constituents of the mixture. Oxidation of the methyl group at C-10 led to the primary alcohols

and then to the corresponding aldehydes, giving origin to the bufotalinin derivatives starting from marinobufagin, resibufagin derivatives from resibufogenin, and hellebrigenin from telocinobufagin, respectively. Further oxidation of the steroid moiety led to alcohol and ketone functions mainly at C-11, C-12, or C-16. The unambiguous identification of the minor constituents requires isolation by preparative HPLC and extensive spectroscopic and spectrometric studies to identify the exact position and stereochemistry of the functional groups. Some differences with the Peruvian *R. marina* are the occurrence of arenobufagin derivatives and a higher number of oxidized compounds in *R. horribilis* compared with the Amazonian species. Interestingly, most of the compounds reported in the *R. horribilis* PGS have been previously described from South American *Rhinella* species [9,10,18] and/or from the crude drug Venenum Bufonis or Ch'an Su from China and Eastern Asia [27,30,31], which exhibit anti-cancer effects in several cancer cell lines [35–40]. Based on this, we propose to evaluate the anti-cancer effect of crude PGS of *R. horribilis* and their fractions A, B, and C.

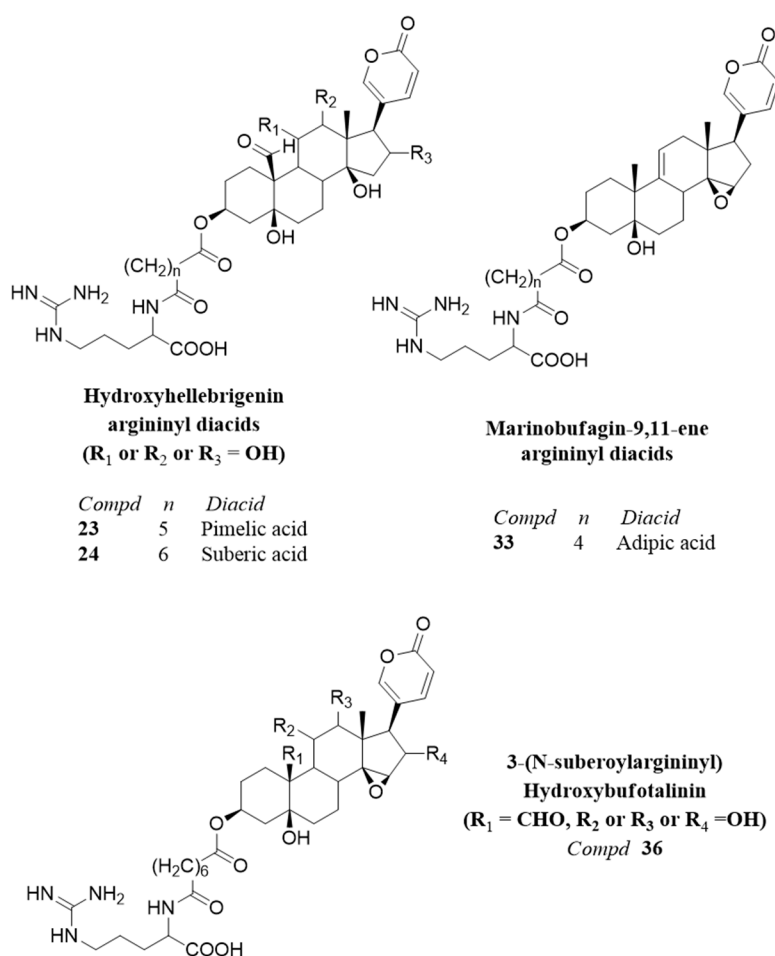


Figure 5. Structure of the compounds 23–24, 33, and 36 tentatively identified in the parotoid gland secretion of *R. horribilis*.

2.4. Effect of *R. horribilis* PGS on Proliferation, Clonogenic Capacity and Reactive Oxygen Species (ROS) Levels of Lung Cancer Cells

To evaluate the anti-proliferative activity of crude PGS (L) of *R. horribilis* and their fractions A, B, and C, lung cancer A549 cells were treated with increasing concentrations by 24 and 48 h and the IC_{50} values were calculated. As Table 2 shows, the crude PGS had an IC_{50} value of $0.031 \pm 0.007 \mu\text{g/mL}$ at 24 h, and fractions A, B, and C were close to 3.08, 4.4, and 1.26 folds more active than crude PGS, respectively and this was a concentration-dependent effect (Figure 6A). At 48 h, fraction C exhibited a strong increase in its anti-proliferative activity.

Table 2. Anti-proliferative effect of fractions A, B, and C and crude extract of parotoid gland secretion of *R. horribilis* on lung cancer A549 cells. Data are expressed as IC₅₀ values (μg/mL ± SEM) of three independent experiments.

Time	Crude Extract	Fraction A	Fraction B	Fraction C
24 h	0.031 ± 0.007	0.010 ± 0.001	0.007 ± 0.001	0.025 ± 0.001
48 h	0.015 ± 0.001 ^a	0.011 ± 0.003	0.006 ± 0.001	0.007 ± 0.002 ^a

^a Significant difference compared to the same fraction (*t*-test two-tailed, IC 95%).

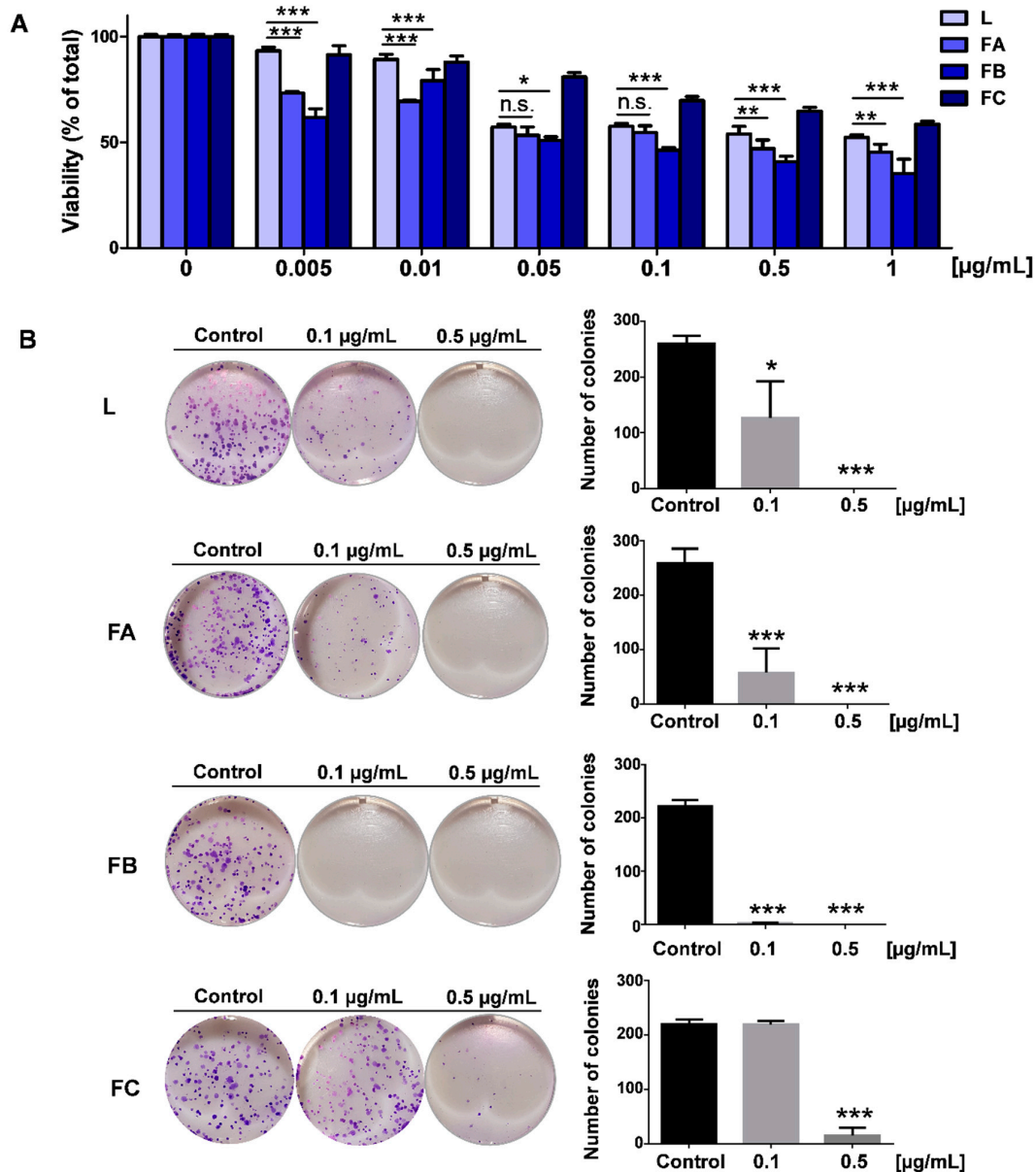


Figure 6. Effect of fractions A, B, C (FA, FB, FC) and crude extract (L) of parotoid gland secretion (PGS) of *R. horribilis* on viability and clonogenic potential of lung cancer A549 cells. (A) Effect of fractions and crude extract on viability at 24 h of exposure. (B) Cells were exposed 24 h to DMSO (control), crude extract (L), and fractions (A, B, and C); then, the culture medium was removed and replaced by fresh medium. The number of colonies was determined at 7 days, using crystal violet staining. Data shown are the mean ± SEM of three independent experiments. * *p* < 0.05, ** *p* < 0.01, *** *p* < 0.001, vs. control (DMSO); n.s., not significant.

The colony formation is the ability of a single cancer cell to proliferate indefinitely, growing into a colony [41]. Since that the concentrations 0.1 and 0.5 $\mu\text{g/mL}$ shown significant differences in viability (Figure 6A), we evaluate if the crude PGS and their fractions A, B, and C irreversibly affect the clonogenic potential of A549 cancer cells. These cells were treated for 24 h with 0.1 and 0.5 $\mu\text{g/mL}$ of crude PGS and their fractions and then, the culture medium was washed and replaced by a fresh and PGS-free culture medium for seven days. As Figure 6B shows, fraction B evoked a strong and irreversible inhibition of the clonogenic potential and fraction C was only active at 0.5 $\mu\text{g/mL}$. Moreover, we evaluate the effect of the *R. horribilis* poison secretion and their fractions on reactive oxygen species (ROS) levels in A549 cancer cells. As Figure 7 shows, all the conditions produced a significant increase in the intracellular ROS levels. Taken together, these results suggest that the PGS of *R. horribilis* increases ROS production and inhibits the proliferation and clonogenic capacity of lung cancer cells, being the fraction B the most active.

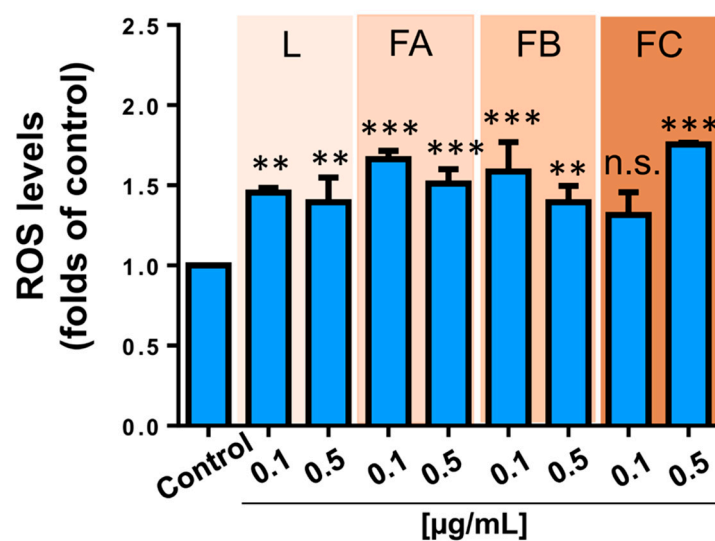


Figure 7. Effect of fractions and crude extract of parotoid gland secretions of *R. horribilis* on ROS production in A549 cancer cells. Cells were exposed 24 h to DMSO (control), crude extract (L), and fractions (A, B, and C), and changes in the ROS levels were determined using dihydroethidium (DHE) probe by flow cytometry. Data shown are the mean \pm SEM of three independent experiments. ** $p < 0.01$, *** $p < 0.001$, vs. control (DMSO). n.s. not significant.

2.5. Effect of *R. horribilis* PGS and Their Fractions on Etoposide-Induced A549 Cell Death

Etoposide (Eto) is a known topoisomerase II inhibitor used in the treatment of several solid cancer, inducing DNA damage, growth arrest, and apoptosis in a concentration-dependent manner [42]. In several cancer cell lines, Eto produces cell cycle arrest in G2-phase [43] through p53 stabilization [44], promoting apoptosis [45]. On the other hand, we have described that the poison secretions of *Rhinella schneideri*, *R. ornata*, and *R. marina* produce G1- or S-phase arrest [9,18], avoiding the cell cycle progression to the G2-phase checkpoint. Therefore, to determine the action of poison secretions of *R. horribilis* on phases of the cell cycle, we evaluate its effect (at 0.5 $\mu\text{g/mL}$) on G2/M arrest-induced cell death by Eto. We hypothesized that whether the *R. horribilis* poison secretion acts on the cell cycle in an earlier phase different to G2/M phase, it will produce a systematic decrease of Eto-induced cell death.

At 48 h of treatment, 25 μM Eto produced $45.50 \pm 1.38\%$ of positive annexin V subpopulation ($p < 0.001$ vs. control), suggesting apoptotic cell death as described [46,47]. As Figure 8 shows, only fraction B induced $22.51 \pm 3.32\%$ of apoptotic cancer cells and crude PGS and other fractions lacked cytotoxic effect. As it was hypothesized, the combination of the *R. horribilis* poison secretion or their fractions plus 25 μM Eto prevented the apoptosis induced by the treatment of only Eto (Figure 8),

suggesting that anti-proliferative effect of the *R. horribilis* poison secretion is produced by cell cycle blocking before of G2/M phase.

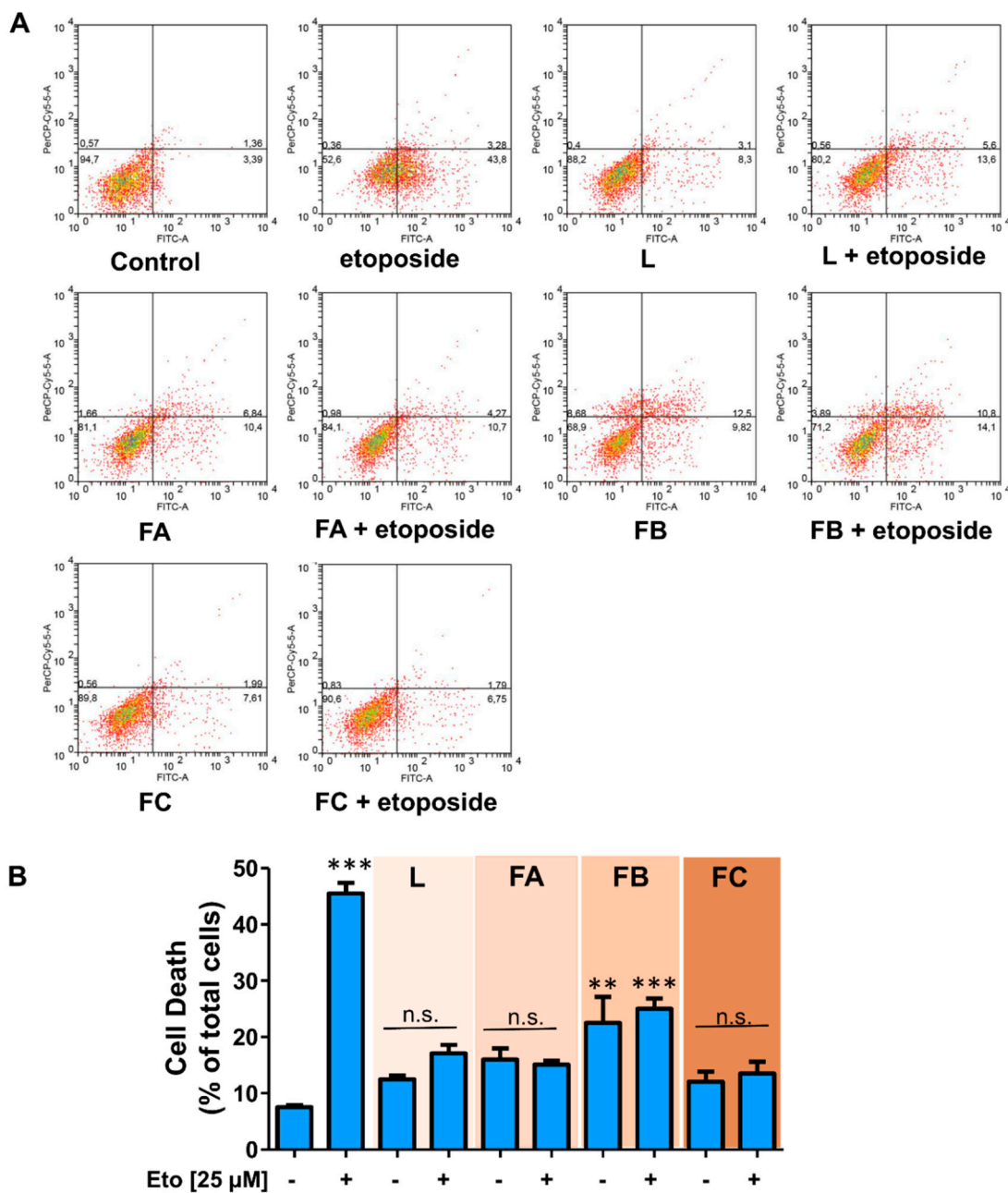


Figure 8. Effect of fractions A, B, C, and crude extract of parotoid gland secretions of *R. horribilis* on etoposide-induced cell death in A549 cancer cells. Cells were exposed 48 h to DMSO (control), crude extract (L), and fractions (FA, FB, and FC) at 0.5 $\mu\text{g}/\text{mL}$ in the presence and absence of 25 μM etoposide (Eto), and viability were determined using Annexin V/PI assay by flow cytometry. (A) Representative dot-plots; (B) quantification. Data shown are the mean \pm SEM of three independent experiments. ** $p < 0.01$, *** $p < 0.001$, vs. control (DMSO). n.s. not significant.

2.6. Effect of Fractions B and C of the *R. horribilis* PGS on the Migration of Lung Cancer Cells

To evaluate the effect of components of *R. horribilis* poison secretion on the migration of cancer cells, we selected both the most active (fraction B) and the less active (fraction C) on inhibition of proliferation. The lung cancer cells were exposed to both fractions by 24 h and the effect on fibronectin-dependent migration was measured. At 0.1 and 0.5 $\mu\text{g}/\text{mL}$, fraction B reduced the migrated cells to 0.79 ± 0.03

and 0.28 ± 0.04 folds of Control and fraction C decreased the migration to 0.95 ± 0.28 and 0.60 ± 0.05 folds of Control, respectively. As Figure 9 shows, fraction B was more active inhibiting the migration of A549 cells.

Although certain bufadienolides present in the poison secretion of toads produce cell cycle arrest in S-phase [48], reduce the activity and protein levels of topoisomerases [49,50] and intercalates with DNA [51]; other DNA damage-independent mechanisms have also been recently described [8,26]. For example, the major constituents of the PGS of *Rhinella* species such as bufalin, marinobufagin, telocinobufagin, and hellebrigenin exhibit strong binding affinities to tubulin in vitro and in vivo conditions, producing dysregulated microtubule arrangement and G2/M cell cycle arrest in cancer cells [8]. In this work, we identified these same tubulin-inhibiting bufadienolides from *R. horribilis* poison secretions and their fractions, producing irreversible inhibition of proliferation and clonogenic capacity, increasing the ROS production, and inhibiting the fibronectin-dependent migration of human lung cancer A549 cells. An interestingly mechanistic explanation of these effects may be proposed, taking into consideration the effects of current MTA on cancer cells mentioned above [16].

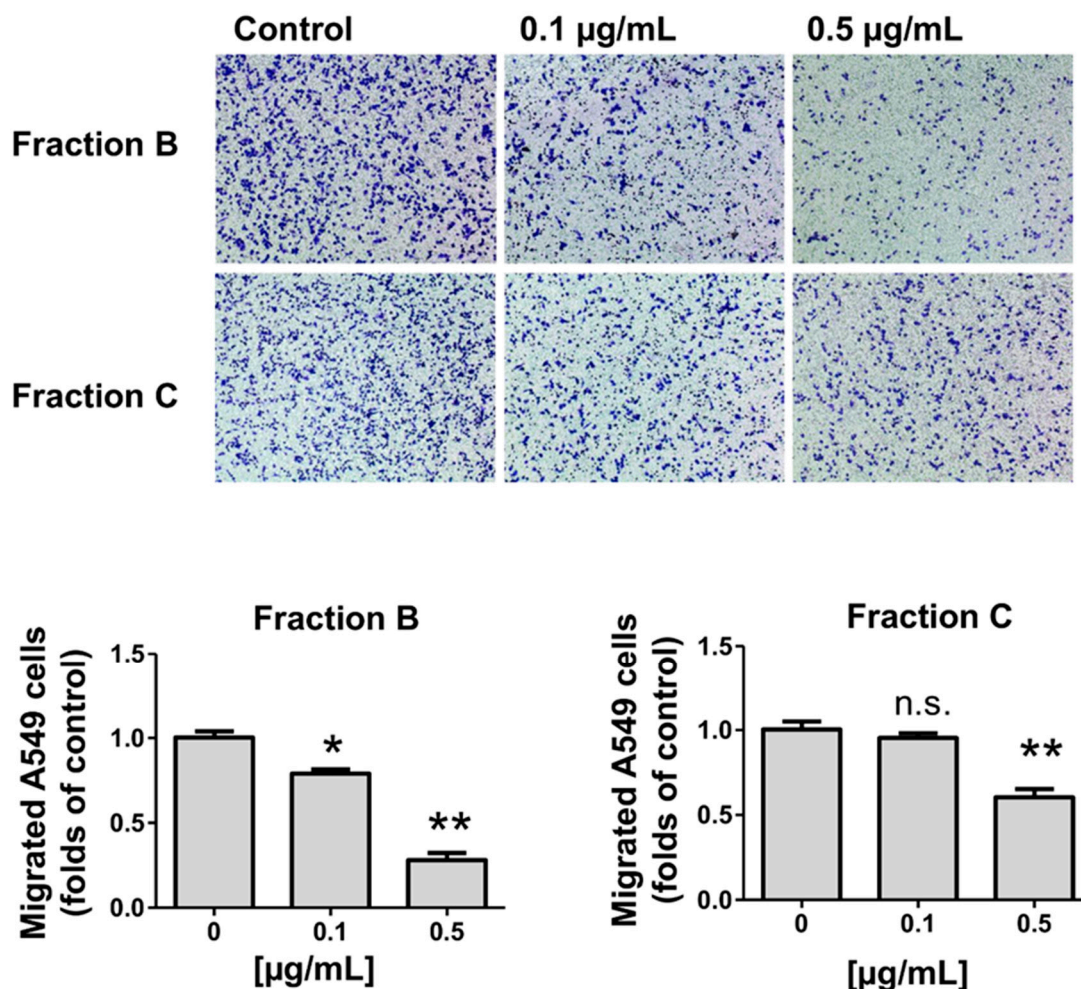


Figure 9. Effect of fractions B and C on fibronectin-dependent migration in A549 cells treated for 24 h. Data shown are the mean \pm SEM of two independent experiments. * $p < 0.05$, ** $p < 0.01$, vs. control (DMSO). n.s. not significant.

3. Conclusions

The composition and biological effects of the PGS of the Amazonian *R. marina* has been extensively studied [8,18,26], while that of *R. horribilis* remained unknown. In this study, some 55 constituents, including argininyl diacids, bufadienolides argininyl diacids, bufadienolides, and alkaloids were

identified/tentatively identified in the PGS of *R. horribilis* for the first time. The number of constituents of this species historically confused with *R. marina* [24], was higher than the 29 compounds reported from three Peruvian Amazon populations of *R. marina* [18].

The alkaloids from the venoms are mainly tryptophan derivatives and some of them present anti-inflammatory effects, as shown by Zhang, et al. [52] on Chinese samples. Several studies on the composition of PGS have been undertaken with the methanol soluble fraction of the crude venom. Recently, the effect was reported of PGS of *Bufo bufo* and *R. marina* on metastatic melanoma, finding that the bufadienolide bufalin was the best antiproliferative agent in the samples [53]. Sinhorin, et al. [54] described the composition of the Amazonian *Rhinella margaritifera* PGS and reported argininyl diacids, bufotalin, and cinobufagin argininyl diacids as well as the bufadienolides bufotalin, cinobufagin, and telocinobufagin as main compounds.

The composition of the PGS in the Peruvian species *R. horribilis* differs from that of *R. margaritifera* by the higher ratio of argininyl diesters, a more complex array of oxidized bufadienolides argininyl diesters, the absence of cinobufagin, and the presence of resibufogenin. When compared with the *Rhinella* species from the Paraguayan river basin area, the toad from the northern Peruvian coast has a much lower content of marinobufagin and its argininyl diacids, that are the main compounds in *R. schneideri* and *R. ornata*, while cinobufagin argininyl diesters are relevant for *R. scitula* [9]. Marinobufagin and its argininyl diesters are the main compounds in *R. marina* from the Peruvian Amazon basin [18]. The chemical composition of the Peruvian coast species shows a different profile that may be associated with a different diet and genetic factors. An update on the chemistry, bioactivity, and quality control of the Asian toad *Bufo gargarizans* has been recently published [55] and provides relevant information to be considered for further studies on the South American species.

Although we describe the anti-cancer effect of the *R. horribilis* PGS, some issues remain to be explored, such as the action of the isolated constituents of crude secretion and the effect on non-tumoral cells and in vivo studies. The *R. horribilis* poison secretions produced irreversible inhibition of proliferation and clonogenic capacity, increasing the ROS production, and inhibiting the fibronectin-dependent migration of human lung cancer A549 cells. The fraction B was the most active on proliferative and migration of cancer cells, suggesting that certain constituents present only in this fraction as minor compounds or the combination of the many different compounds acting in synergy may be attractive candidates for further anti-cancer studies.

4. Materials and Methods

4.1. Parotid Glands Secretions (PGS) Samples

Twenty female *Rhinella horribilis* (Wiegmann, 1833) toads were collected in the Region of Piura, on the north coast of Peru, between December 2018 to January 2019 with herpetologists from Universidad Nacional de Trujillo. The size and weight of the animals ranged between 15.2 to 19.8 cm and 145 to 310 g, respectively. The animals were gently placed in cardboard boxes and then transferred to the Pharmacognosy Laboratory of Universidad Nacional de Trujillo, Peru. The skin secretions were obtained by mild electric stimulation using platinum electrodes (4-ms pulse width, 50 Hz, 5V) (Memex) by ten seconds, as described by Thirupathi, et al. [56]. Next, the parotid glands of the toads were gently pressed with the hands to remove the PGS, which was placed in a beaker. All animals were released after collecting the samples. The fresh PGS (5.4 g) was resuspended in MeOH and was sonicated for 5 min, filtered, taken to dryness under reduced pressure, and lyophilized, affording 900 mg of the crude extract of PGS. The *w/w* extraction yield of the MeOH extract was 16.7%.

The obtention of peptides from the toad venom needs a different protocol than that used in our work. The venoms should be extracted with a saline buffer [22] or with acidified water and not with organic solvents. The clean-up requires methods used for protein isolation and identification. The identification of the peptides also requires different analytical tools, MALDI-TOF detection, microsequencing, and synthesis [23].

4.2. Thin-Layer Chromatography Analysis

For the thin-layer chromatography (TLC) analysis, commercial plates coated with silica gel F₂₅₄ as the stationary phase were used. For visualization of the TLC profile, the plates were first observed immediately after the TLC at wavelengths (λ) 254 and 365 nm. Afterward, the plates were sprayed with a *p*-anisaldehyde solution reagent freshly prepared (2.0 mL *p*-anisaldehyde in 340 mL ethanol, 40 mL glacial acetic acid, and 20 mL 97% sulfuric acid) followed by heating up to 105 °C for maximum visualization of spots.

4.3. HPLC-DAD Analysis

The system used was a Shimadzu[®] Prominence (Shimadzu Corporation, Kyoto, Japan) consisting of a LC-20AT pump, a SPD-M20A UV diode array detector, CTO-20 AC column oven, and a LabSolutions software (Version 5.51, Shimadzu Corporation, Kyoto, Japan). A MultoHigh 100 RP 18, 5 μ column (250 \times 4.6 mm) (CS—Chromatographie Service GmbH, Langerwehe, Germany) was used. The temperature was set at 30 °C. The HPLC analyses were performed using a linear gradient solvent system consisting of methanol:acetonitrile 50:50 (A) and 0.1% formic acid in water (B) with a flow rate of 0.4 mL/min as follows: initial conditions were 8% A and 92% B; 0–10 min: 92% to 85% B; 10–25 min: 85% to 70% B; 25–35 min: 70% to 65% B; 35–45 min: 65% to 55% B; 45–55 min: 55% to 50% B; 55 to 75 min: 50% to 45% B; 75 to 95 min: 45% to 35% B; 95 to 100 min: 35% to 25% B; 100 to 105 min: 25% B; 105 to 110 min: 25% to 40% B; 110 to 120 min: 40% to 60% B; 120 to 130 min: 60% to 75% B; 130 to 135 min: 75% to 92% B; 135 to 145 min: back to 92% B (initial condition). The volume injected was 20 μ L. The compounds were monitored at 254, 280, and 330 nm. UV spectra of the compounds detected were recorded from 200 to 500 nm for peak characterization.

4.4. HPLC-DAD-Q-TOF-MS/MS Analysis

HPLC-DAD-MS/MS analysis was performed using a UHPLC/HPLC-DAD Bruker Elute LC system coupled in tandem with a Q-TOF Compact (Bruker Daltonik, Bremen, Germany). The same above-mentioned reverse phase column and a linear gradient solvent system (HPLC-DAD analysis, Section 4.3) were performed. The volume injected was 5 μ L of a 10 mg/mL solution.

The data were acquired in the full scan mode (range of *m/z* 50–1500) in positive electrospray ionization mode using capillary voltage at 4.5 kV; nebulizer and drying gas (N₂) at 4.0 bar and 9.0 L/min, respectively; dry temperature of 200 °C. The MS/MS spectra were acquired in auto mode using variable collision energy of 250 to 100% of 10 eV. Internal calibration of the instrument was accomplished using 10 mM sodium formate solution introduced to the ion source via a 20 μ L loop at the beginning of each analysis. The compounds were identified by comparison of the fragmentation pattern, UV profile, and mass spectra.

4.5. NMR Analysis

The NMR spectra were recorded on a Bruker Avance 400 spectrometer (Bruker, Rheinstetten, Germany) at 400 MHz for ¹H and 100 MHz for ¹³C in CD₃OD. Chemical shifts are given in ppm with residual methanol as the internal standard.

4.6. Cell Culture Conditions

Human lung cancer A549 cells were grown in Dulbecco's modified Eagle's medium (DMEM), containing 25 mM glucose and 4 mM glutamine supplemented with 10% fetal bovine serum (FBS), penicillin (100 IU/mL), and streptomycin (100 μ g/mL). No exogenous pyruvate supplementation was added, and cells were maintained in a humidified atmosphere at 37 °C and 5% CO₂.

4.7. Colony Formation

For the colony assay, A549 cells were seeded in 6-well plates at 500 cells per well according to Franken et al. [41] and incubated for 24 h. The cells were treated with the crude extract (L) and fractions A, B and, C of *R. horribilis* secretions for 24 h. After treatment, the medium was replaced with fresh medium, and the cells were incubated for 7 days to allow colony formation. Colonies were stained with 0.5% crystal violet solution in 20% methanol and washed with tap water. Colony formation was analyzed with ImageJ software (NIH, Bethesda, MD, USA) as we described [57].

4.8. Determination of ROS Levels

The generation of intracellular oxidative stress was determined using the dihydroethidium (DHE) probe as previously described [58]. In brief, A549 cells were grown in complete media, seeded in 12-well plates (50,000 cells/mL) allowed overnight to attach. Cells were exposed for 24 h to DMSO (Control) or 0.1 and 0.5 µg/mL of crude poison secretion (L) or A, B, and C fractions. Then, culture media was replaced by a solution containing 5 µM DHE in Hank's balanced salt solution (HBSS) and incubated for 20 min in the dark. After this time, cells were washed, trypsinized, and resuspended in 200 µL of HBSS and measured by FACSCanto flow cytometer.

4.9. Migration Assay

Cell migration was evaluated in Boyden Chamber assays (Transwell Costar, 6.5-mm diameter, 8-µm pore size) as previously reported [58]. The cancer cells were exposed to fractions B and C (0.1 and 0.5 µg/mL) for 24 h. Then, cancer cells (50,000 cells/mL) were re-suspended in serum-free medium, plated on top of the chamber insert coated with fibronectin (2 µg/mL), and incubated at 37 °C for 2 h. The inserts were removed, washed, and the bottom side of the inserts was stained with 0.5% crystal violet solution in 20% methanol. Cells from eight different frames were counted for each condition in an inverted microscope.

4.10. Annexin V/Propidium Iodide Staining

The cell death was evaluated using annexin V/propidium iodide (AV/PI) dual staining, following the instructions of the Annexin V-FITC Apoptosis Detection Kit (Abcam, Cambridge, UK), as previously reported [57]. In brief, A549 cancer cells were seeded (50,000 cells/mL) in 12-well plates, treated with 0.5 µg/mL of the crude extract (L) and fractions for 24 h. The fluorescence was measured by flow cytometry.

4.11. Statistics Analysis

All statistical analyses were performed using Graph Pad Prism 4.03 (GraphPad Software, San Diego, California, USA). The data are expressed as mean ± SEM of three independent experiments. Statistical analysis was performed using one-way or two-way ANOVA with Bonferroni's post-test for pairwise comparisons. The data were considered statistically significant when $p < 0.05$.

Author Contributions: Conceptualization, G.S.-H., J.P.d.A., M.R.S.-V., P.A.A.A.-G. and F.A.U.; investigation, J.P.d.A., M.R.S.-V., P.A.A.A.-G., C.P., S.F.-R., M.M. and P.C.; writing—original draft preparation, G.S.-H. and F.A.U.; writing—review and editing, G.S.-H. and F.A.U. All authors have read and agreed to the published version of the manuscript.

Funding: This work was supported by ANID PCI-Biotechnology #Redbio0027, FONDEQUIP EQM 170023, and "líneas de apoyo a la investigación financiadas por ICBM (2020)". J.P.de A. thanks the Universidad de Talca for a Postdoctoral grant and CP thanks ANID for Master fellowship #22191223.

Conflicts of Interest: The authors declare no conflict of interest.

References

1. Catenazzi, A.; Lehr, E.; May, R.V. The amphibians and reptiles of Manu National Park and its buffer zone, Amazon basin and eastern slopes of the Andes, Peru. *Biota Neotrop.* **2013**, *13*, 269–283. [[CrossRef](#)]
2. Moravec, J.; Lehr, E.; Cusi, J.C.; Córdova, J.H.; Gvoždík, V. A new species of the *Rhinella margaritifera* species group (Anura, Bufonidae) from the montane forest of the Selva Central, Peru. *Zookeys* **2014**, 35–56. [[CrossRef](#)]
3. Pejic, R.; Simic Prskalo, M.; Simic, J. Ocular Hypotonia and Transient Decrease of Vision as a Consequence of Exposure to a Common Toad Poison. *Case Rep. Ophthalmol. Med.* **2020**, *2020*, 2983947. [[CrossRef](#)]
4. Isoardi, K.; Lee, S.; Burren, J.M.; George, J.; Goggin, A.; Chan, B.S. Bufadienolide toxicity in a child following cane toad egg ingestion. *Emerg. Med. Australas.* **2018**, *30*, 728–729. [[CrossRef](#)]
5. Peterson, M.E.; Roberts, B.K. Toads. In *Small Animal Toxicology*, 3rd ed.; Peterson, M.E., Talcott, P.A., Eds.; Elsevier: Amsterdam, The Netherlands, 2013; pp. 833–839.
6. McClelland, D. The Moche Botanical Frog. *Arqueol. Iberoam.* **2011**, *10*, 30–42. [[CrossRef](#)]
7. Donnan, C.B. *Moche Art of Peru*; Museum of Cultural Heritage, University of California: Los Angeles, CA, USA, 1978; p. 205.
8. Abdelfatah, S.; Lu, X.; Schmeda-Hirschmann, G.; Efferth, T. Cytotoxicity and antimitotic activity of *Rhinella schneideri* and *Rhinella marina* venoms. *J. Ethnopharmacol.* **2019**, *242*, 112049. [[CrossRef](#)] [[PubMed](#)]
9. Schmeda-Hirschmann, G.; Gomez, C.V.; Rojas de Arias, A.; Burgos-Edwards, A.; Alfonso, J.; Rolon, M.; Brusquetti, F.; Netto, F.; Urra, F.A.; Cárdenas, C. The Paraguayan *Rhinella* toad venom: Implications in the traditional medicine and proliferation of breast cancer cells. *J. Ethnopharmacol.* **2017**, *199*, 106–118. [[CrossRef](#)] [[PubMed](#)]
10. Schmeda-Hirschmann, G.; Quispe, C.; Theoduloz, C.; de Sousa, P.T., Jr.; Parizotto, C. Antiproliferative activity and new argininyl bufadienolide esters from the “cururú” toad *Rhinella (Bufo) schneideri*. *J. Ethnopharmacol.* **2014**, *155*, 1076–1085. [[CrossRef](#)] [[PubMed](#)]
11. Indini, A.; Rijavec, E.; Bareggi, C.; Grossi, F. Novel treatment strategies for early-stage lung cancer: The oncologist’s perspective. *J. Thorac. Dis.* **2020**, *12*, 3390–3398. [[CrossRef](#)] [[PubMed](#)]
12. Majem, B.; Nadal, E.; Muñoz-Pinedo, C. Exploiting metabolic vulnerabilities of Non small cell lung carcinoma. *Semin. Cell Dev. Biol.* **2020**, *98*, 54–62. [[CrossRef](#)] [[PubMed](#)]
13. Rigas, J.R. Taxane-platinum combinations in advanced non-small cell lung cancer: A review. *Oncologist* **2004**, *9* (Suppl. S2), 16–23. [[CrossRef](#)]
14. Frisone, D.; Friedlaender, A.; Malapelle, U.; Banna, G.; Addeo, A. A BRAF new world. *Crit. Rev. Oncol. Hematol.* **2020**, *152*, 103008. [[CrossRef](#)] [[PubMed](#)]
15. Gandolovičová, A.; Rosel, D.; Fernandes, M.; Veselý, P.; Heneberg, P.; Čermák, V.; Petruželka, L.; Kumar, S.; Sanz-Moreno, V.; Brábek, J. Migrastatics-Anti-metastatic and Anti-invasion Drugs: Promises and Challenges. *Trends Cancer* **2017**, *3*, 391–406. [[CrossRef](#)] [[PubMed](#)]
16. Čermák, V.; Dostál, V.; Jelínek, M.; Libusová, L.; Kovář, J.; Rösel, D.; Brábek, J. Microtubule-targeting agents and their impact on cancer treatment. *Eur. J. Cell Biol.* **2020**, *99*, 151075. [[CrossRef](#)] [[PubMed](#)]
17. Sciani, J.M.; Angeli, C.B.; Antoniazzi, M.M.; Jared, C.; Pimenta, D.C. Differences and similarities among parotoid macrogland secretions in South American toads: A preliminary biochemical delineation. *Sci. World J.* **2013**, *2013*, 937407. [[CrossRef](#)]
18. Schmeda-Hirschmann, G.; Quispe, C.; Arana, G.V.; Theoduloz, C.; Urra, F.A.; Cárdenas, C. Antiproliferative activity and chemical composition of the venom from the Amazonian toad *Rhinella marina* (Anura: Bufonidae). *Toxicon* **2016**, *121*, 119–129. [[CrossRef](#)]
19. Sousa, L.Q.; Machado, K.D.; Oliveira, S.F.; Araújo, L.D.; Monção-Filho, E.D.; Melo-Cavalcante, A.A.; Vieira-Júnior, G.M.; Ferreira, P.M. Bufadienolides from amphibians: A promising source of anticancer prototypes for radical innovation, apoptosis triggering and Na(+)/K(+)-ATPase inhibition. *Toxicon* **2017**, *127*, 63–76. [[CrossRef](#)]
20. Tornesello, A.L.; Borrelli, A.; Buonaguro, L.; Buonaguro, F.M.; Tornesello, M.L. Antimicrobial peptides as anticancer agents: Functional properties and biological activities. *Molecules* **2020**, *25*, 2850. [[CrossRef](#)]
21. Kunda, N.K. Antimicrobial peptides as novel therapeutics for non-small cell lung cancer. *Drug Discov. Today* **2020**, *25*, 238–247. [[CrossRef](#)]
22. Xia, F.; Gao, F.; Yao, H.; Zhang, G.; Gao, B.; Lu, Y.; Wang, X.; Qian, Y. Identification of angiogenesis-inhibiting peptides from Chan Su. *Protein Expr. Purif.* **2019**, *163*, 105445. [[CrossRef](#)]

23. Han, Y.; Lu, M.; Zhou, J. Buforin IIb induces androgen-independent prostate cancer cells apoptosis through p53 pathway in vitro. *Toxicon* **2019**, *168*, 16–21. [[CrossRef](#)] [[PubMed](#)]
24. Acevedo, A.A.; Lampo, M.; Cipriani, R. The cane or marine toad, *Rhinella marina* (Anura, Bufonidae): Two genetically and morphologically distinct species. *Zootaxa* **2016**, *4103*, 574–586. [[CrossRef](#)] [[PubMed](#)]
25. Orihuela-Torres, A.; Ordóñez-Delgado, L.; Brito, J.; López, F.; Mazón, M.; Freile, J.F. Feeding ecology of the Burrowing Owl *Athene cunicularia punensis* (Strigiformes: Strigidae) in the Jambelí archipelago, El Oro province, southwestern Ecuador. *Rev. Peru. Biol.* **2018**, *25*, 123–130. [[CrossRef](#)]
26. de Medeiros, D.S.S.; Rego, T.B.; Dos Santos, A.P.A.; Pontes, A.S.; Moreira-Dill, L.S.; Matos, N.B.; Zuliani, J.P.; Stábeli, R.G.; Teles, C.B.G.; Soares, A.M.; et al. Biochemical and Biological profile of parotoid secretion of the Amazonian *Rhinella marina* (Anura: Bufonidae). *Biomed. Res. Int.* **2019**, *2019*, 2492315. [[CrossRef](#)] [[PubMed](#)]
27. Kamano, Y.; Nogawa, T.; Yamashita, A.; Pettit, G. The ¹H and ¹³C NMR chemical shift assignments for thirteen bufadienolides isolated from the traditional Chinese drug Ch’an Su. *Collect. Czechoslov. Chem. Commun.* **2001**, *66*, 1841–1848. [[CrossRef](#)]
28. Cao, Y.; Wu, J.; Pan, H.; Wang, L. Chemical profile and multicomponent quantitative analysis for the quality evaluation of toad venom from different origins. *Molecules* **2019**, *24*, 3595. [[CrossRef](#)] [[PubMed](#)]
29. Ye, M.; Guo, D.A. Analysis of bufadienolides in the Chinese drug ChanSu by high-performance liquid chromatography with atmospheric pressure chemical ionization tandem mass spectrometry. *Rapid Commun. Mass Spectrom.* **2005**, *19*, 1881–1892. [[CrossRef](#)] [[PubMed](#)]
30. Wei, W.L.; Hou, J.J.; Wang, X.; Yu, Y.; Li, H.J.; Li, Z.W.; Feng, Z.J.; Qu, H.; Wu, W.Y.; Guo, D.A. Venenum bufonis: An overview of its traditional use, natural product chemistry, pharmacology, pharmacokinetics and toxicology. *J. Ethnopharmacol.* **2019**, *237*, 215–235. [[CrossRef](#)] [[PubMed](#)]
31. Zhang, Y.; Jin, H.; Li, X.; Zhao, J.; Guo, X.; Wang, J.; Guo, Z.; Zhang, X.; Tao, Y.; Liu, Y.; et al. Separation and characterization of bufadienolides in toad skin using two-dimensional normal-phase liquid chromatography×reversed-phase liquid chromatography coupled with mass spectrometry. *J. Chromatogr. B Anal. Technol. Biomed. Life Sci.* **2016**, *1026*, 67–74. [[CrossRef](#)]
32. Liu, Y.; Xiao, Y.; Xue, X.; Zhang, X.; Liang, X. Systematic screening and characterization of novel bufadienolides from toad skin using ultra-performance liquid chromatography/electrospray ionization quadrupole time-of-flight mass spectrometry. *Rapid Commun. Mass Spectrom.* **2010**, *24*, 667–678. [[CrossRef](#)] [[PubMed](#)]
33. Ren, W.; Han, L.; Luo, M.; Bian, B.; Guan, M.; Yang, H.; Han, C.; Li, N.; Li, T.; Li, S.; et al. Multi-component identification and target cell-based screening of potential bioactive compounds in toad venom by UPLC coupled with high-resolution LTQ-Orbitrap MS and high-sensitivity Qtrap MS. *Anal. Bioanal. Chem.* **2018**, *410*, 4419–4435. [[CrossRef](#)] [[PubMed](#)]
34. Bessa-Silva, A.; Vallinoto, M.; Sampaio, I.; Flores-Villela, O.A.; Smith, E.N.; Sequeira, F. The roles of vicariance and dispersal in the differentiation of two species of the *Rhinella marina* species complex. *Mol. Phylogenet. Evol.* **2020**, *145*, 106723. [[CrossRef](#)] [[PubMed](#)]
35. Kamano, Y.; Yamashita, A.; Nogawa, T.; Morita, H.; Takeya, K.; Itokawa, H.; Segawa, T.; Yukita, A.; Saito, K.; Katsuyama, M.; et al. QSAR evaluation of the Ch’an Su and related bufadienolides against the colchicine-resistant primary liver carcinoma cell line PLC/PRF/5(1). *J. Med. Chem.* **2002**, *45*, 5440–5447. [[CrossRef](#)] [[PubMed](#)]
36. Nogawa, T.; Kamano, Y.; Yamashita, A.; Pettit, G.R. Isolation and structure of five new cancer cell growth inhibitory bufadienolides from the Chinese traditional drug Ch’an Su. *J. Nat. Prod.* **2001**, *64*, 1148–1152. [[CrossRef](#)]
37. Xu, R.; Xie, H.Q.; Deng, L.L.; Zhang, J.X.; Yang, F.M.; Liu, J.H.; Hao, X.J.; Zhang, Y.H. A new bufadienolide with cytotoxic activity from the Chinese traditional drug Ch’an Su. *Chin. J. Nat. Med.* **2014**, *12*, 623–627. [[CrossRef](#)]
38. Kim, N.Y.; Suh, Y.A.; Kim, S.; Lee, C. Bufalin down-regulates Axl expression to inhibit cell proliferation and induce apoptosis in non-small-cell lung cancer cells. *Biosci. Rep.* **2020**, *40*. [[CrossRef](#)]

39. Wang, J.; Cai, H.; Liu, Q.; Xia, Y.; Xing, L.; Zuo, Q.; Zhang, Y.; Chen, C.; Xu, K.; Yin, P.; et al. Cinobufacini Inhibits Colon Cancer Invasion and Metastasis via Suppressing Wnt/ β -Catenin Signaling Pathway and EMT. *Am. J. Chin. Med.* **2020**, *48*, 703–718. [[CrossRef](#)]
40. Zhao, J.; Zhang, Q.; Zou, G.; Gao, G.; Yue, Q. Arenobufagin, isolated from toad venom, inhibited epithelial-to-mesenchymal transition and suppressed migration and invasion of lung cancer cells via targeting IKK β /NF κ B signal cascade. *J. Ethnopharmacol.* **2020**, *250*, 112492. [[CrossRef](#)]
41. Franken, N.A.; Rodermond, H.M.; Stap, J.; Haveman, J.; van Bree, C. Clonogenic assay of cells in vitro. *Nat. Protoc.* **2006**, *1*, 2315–2319. [[CrossRef](#)]
42. Jeyapalan, J.; Leake, A.; Ahmed, S.; Saretzki, G.; Tilby, M.; von Zglinicki, T. The role of telomeres in Etoposide induced tumor cell death. *Cell Cycle* **2004**, *3*, 1169–1176. [[CrossRef](#)]
43. Jain, C.K.; Roychoudhury, S.; Majumder, H.K. Selective killing of G2 decatenation checkpoint defective colon cancer cells by catalytic topoisomerase II inhibitor. *Biochim. Biophys. Acta* **2015**, *1853*, 1195–1204. [[CrossRef](#)] [[PubMed](#)]
44. Clifford, B.; Beljin, M.; Stark, G.R.; Taylor, W.R. G2 arrest in response to topoisomerase II inhibitors: The role of p53. *Cancer Res.* **2003**, *63*, 4074–4081.
45. Chiu, C.C.; Li, C.H.; Ung, M.W.; Fuh, T.S.; Chen, W.L.; Fang, K. Etoposide (VP-16) elicits apoptosis following prolonged G2-M cell arrest in p53-mutated human non-small cell lung cancer cells. *Cancer Lett.* **2005**, *223*, 249–258. [[CrossRef](#)]
46. Ceballos-Cancino, G.; Espinosa, M.; Maldonado, V.; Melendez-Zajgla, J. Regulation of mitochondrial Smac/DIABLO-selective release by survivin. *Oncogene* **2007**, *26*, 7569–7575. [[CrossRef](#)] [[PubMed](#)]
47. Meresse, P.; Dechaux, E.; Monneret, C.; Bertounesque, E. Etoposide: Discovery and medicinal chemistry. *Curr. Med. Chem.* **2004**, *11*, 2443–2466. [[CrossRef](#)] [[PubMed](#)]
48. Ma, L.; Song, B.; Jin, H.; Pi, J.; Liu, L.; Jiang, J.; Cai, J. Cinobufacini induced MDA-MB-231 cell apoptosis-associated cell cycle arrest and cytoskeleton function. *Bioorg. Med. Chem. Lett.* **2012**, *22*, 1459–1463. [[CrossRef](#)]
49. Hashimoto, S.; Jing, Y.; Kawazoe, N.; Masuda, Y.; Nakajo, S.; Yoshida, T.; Kuroiwa, Y.; Nakaya, K. Bufalin reduces the level of topoisomerase II in human leukemia cells and affects the cytotoxicity of anticancer drugs. *Leuk. Res.* **1997**, *21*, 875–883. [[CrossRef](#)]
50. Liu, Y.; Ban, L.Y.; Su, X.; Gao, S.; Liu, J.W.; Cui, X.N. Effects of cinobufacini injection on cell proliferation and the expression of topoisomerases in human HepG-2 hepatocellular carcinoma cells. *Mol. Med. Rep.* **2015**, *12*, 1598–1604. [[CrossRef](#)] [[PubMed](#)]
51. Deng, L.J.; Peng, Q.L.; Wang, L.H.; Xu, J.; Liu, J.S.; Li, Y.J.; Zhuo, Z.J.; Bai, L.L.; Hu, L.P.; Chen, W.M.; et al. Arenobufagin intercalates with DNA leading to G2 cell cycle arrest via ATM/ATR pathway. *Oncotarget* **2015**, *6*, 34258–34275. [[CrossRef](#)]
52. Zhang, Y.; Yuan, B.; Takagi, N.; Wang, H.; Zhou, Y.; Si, N.; Yang, J.; Wei, X.; Zhao, H.; Bian, B. Comparative analysis of hydrophilic ingredients in toad skin and toad venom using the UHPLC-HR-MS/MS and UPLC-QqQ-MS/MS methods together with the anti-inflammatory evaluation of indolealkylamines. *Molecules* **2018**, *24*, 86. [[CrossRef](#)]
53. Soumoy, L.; Wells, M.; Najem, A.; Krayem, M.; Ghanem, G.; Hambye, S.; Saussez, S.; Blankert, B.; Journe, F. Toad venom antiproliferative activities on metastatic melanoma: Bio-guided fractionation and screening of the compounds of two different venoms. *Biology* **2020**, *9*, 218. [[CrossRef](#)] [[PubMed](#)]
54. Sinhorin, A.P.; Kerkhoff, J.; Dall'Oglio, E.L.; de Jesus Rodrigues, D.; de Vasconcelos, L.G.; Sinhorin, V.D.G. Chemical profile of the parotoid gland secretion of the Amazonian toad (*Rhinella margaritifera*). *Toxicon* **2020**, *182*, 30–33. [[CrossRef](#)] [[PubMed](#)]
55. Zhan, X.; Wu, H.; Wu, H.; Wang, R.; Luo, C.; Gao, B.; Chen, Z.; Li, Q. Metabolites from *Bufo gargarizans* (Cantor, 1842): A review of traditional uses, pharmacological activity, toxicity and quality control. *J. Ethnopharmacol.* **2020**, *246*, 112178. [[CrossRef](#)] [[PubMed](#)]
56. Thirupathi, K.; Chandrakala, G.; Krishna, L.; Bheem Rao, T.; Venkaiah, Y. Antibacterial activity of skin secretion and its extraction from the toad *Bufo melanostictus*. *Eur. J. Pharm. Med Res.* **2018**, *3*, 283–286.

57. Fuentes-Retamal, S.; Sandoval-Acuna, C.; Peredo-Silva, L.; Guzman-Rivera, D.; Pavani, M.; Torrealba, N.; Truksa, J.; Castro-Castillo, V.; Catalan, M.; Kemmerling, U.; et al. Complex Mitochondrial Dysfunction Induced by TPP(+)-Gentisic Acid and Mitochondrial Translation Inhibition by Doxycycline Evokes Synergistic Lethality in Breast Cancer Cells. *Cells* **2020**, *9*, 407. [[CrossRef](#)]
58. Urra, F.A.; Munoz, F.; Cordova-Delgado, M.; Ramirez, M.P.; Pena-Ahumada, B.; Rios, M.; Cruz, P.; Ahumada-Castro, U.; Bustos, G.; Silva-Pavez, E.; et al. FR58P1a; a new uncoupler of OXPHOS that inhibits migration in triple-negative breast cancer cells via Sirt1/AMPK/beta1-integrin pathway. *Sci. Rep.* **2018**, *8*, 13190. [[CrossRef](#)]



© 2020 by the authors. Licensee MDPI, Basel, Switzerland. This article is an open access article distributed under the terms and conditions of the Creative Commons Attribution (CC BY) license (<http://creativecommons.org/licenses/by/4.0/>).